Elabela/Toddler Is an Endogenous Agonist of the Apelin APJ Receptor in the Adult Cardiovascular System, and Exogenous Administration of the Peptide Compensates for the Downregulation of Its Expression in Pulmonary Arterial Hypertension

BACKGROUND: Elabela/toddler (ELA) is a critical cardiac developmental peptide that acts through the G-protein–coupled apelin receptor, despite lack of sequence similarity to the established ligand apelin. Our aim was to investigate the receptor pharmacology, expression pattern, and in vivo function of ELA peptides in the adult cardiovascular system, to seek evidence for alteration in pulmonary arterial hypertension (PAH) in which apelin signaling is downregulated, and to demonstrate attenuation of PAH severity with exogenous administration of ELA in a rat model.

METHODS: In silico docking analysis, competition binding experiments, and downstream assays were used to characterize ELA receptor binding in human heart and signaling in cells expressing the apelin receptor. ELA expression in human cardiovascular tissues and plasma was determined using real-time quantitative polymerase chain reaction, dual-labeling immunofluorescent staining, and immunoassays. Acute cardiac effects of ELA-32 and [Pyr^{1}] apelin-13 were assessed by MRI and cardiac catheterization in anesthetized rats. Cardiopulmonary human and rat tissues from PAH patients and monocrotaline- and Sugen/hypoxia-exposed rats were used to show changes in ELA expression in PAH. The effect of ELA treatment on cardiopulmonary remodeling in PAH was investigated in the monocrotaline rat model.

RESULTS: ELA competed for binding of apelin in human heart with overlap for the 2 peptides indicated by *in silico* modeling. ELA activated G-protein– and β-arrestin–dependent pathways. We detected ELA expression in human vascular endothelium and plasma. Comparable to apelin, ELA increased cardiac contractility, ejection fraction, and cardiac output and elicited vasodilatation in rat in vivo. ELA expression was reduced in cardiopulmonary tissues from PAH patients and PAH rat models, respectively. ELA treatment significantly attenuated elevation of right ventricular systolic pressure and right ventricular hypertrophy and pulmonary vascular remodeling in monocrotaline-exposed rats.

CONCLUSIONS: These results show that ELA is an endogenous agonist of the human apelin receptor, exhibits a cardiovascular profile comparable to apelin, and is downregulated in human disease and rodent PAH models, and exogenous peptide can reduce the severity of cardiopulmonary remodeling and function in PAH in rats. This study provides additional proof of principle that an apelin receptor agonist may be of therapeutic use in PAH in humans.

Peiran Yang, MA
Cai Read, MRes
Rhoda E. Kuc, BA
Guido Buonincontri, PhD
Mark Southwood, PhD
Rubben Torella, PhD
Paul D. Upton, PhD
Alexi Crosby, PhD
Stephen J. Sawiak, PhD
T. Adrian Carpenter, PhD
Robert C. Glen, PhD
Nicholas W. Morrell, MD
Janet J. Maguire, PhD*
Anthony P. Davenport, PhD*

*Drs Maguire and Davenport share joint last authorship.

Correspondence to:
Anthony P. Davenport, PhD, Experimental Medicine and Immunotherapeutics, University of Cambridge, Level 6, Centre for Clinical Investigation, Box 110, Addenbrooke's Hospital, Cambridge, CB2 0QQ, UK. E-mail apd10@medschl.cam.ac.uk

Sources of Funding, see page 1172

Key Words: apelin ■ cardiopulmonary ■ Elabela/Toddler ■ pulmonary hypertension ■ receptors, G-protein-coupled

Clinical Perspective

What Is New?

- Elabela/toddler (ELA) was first identified as an essential peptide in the development of the heart in zebrafish, and proposed as a second endogenous ligand at the apelin receptor.
- We have now shown that ELA is widely expressed in the adult human cardiovascular system, localizing to the vascular endothelium and plasma.
- ELA peptides activated G-protein– and β-arrestin–dependent pathways with comparable potency to apelin and, crucially, these actions were blocked by apelin receptor antagonists.
- ELA increased cardiac contractility, ejection fraction, and cardiac output, and it elicited vasodilatation in anesthetized rats in vivo.

What Are the Clinical Implications?

- Apelin is known to be downregulated in human and animal models of pulmonary arterial hypertension (PAH).
- We have demonstrated that ELA did not compensate for the loss of apelin, because its expression was also significantly reduced in cardiopulmonary tissues from human PAH patients and in rat models of PAH.
- Treatment with exogenous ELA attenuated right ventricular hypertrophy, systolic pressure, and pulmonary vascular remodeling in the monocrotaline rat model of PAH.
- The results suggest that a selective first-in-class agonist that mimics the action of the endogenous ligands apelin/ELA is a promising therapeutic strategy in the treatment of PAH distinct from pathways targeted by current clinical treatments.

The apelin family of peptides interacts with a G-protein–coupled receptor named the apelin receptor or APJ. Apelin peptides have an emerging role in the adult cardiovascular system[1] and in embryonic development of the heart,[2] and [Pyr1]apelin-13 is the most abundant endogenous apelin peptide in the human heart.[3] Alteration in the apelin system is thought to contribute to the etiology of cardiovascular diseases such as pulmonary arterial hypertension (PAH), a devastating disease with pulmonary vascular remodeling leading to death from right ventricular failure in which a beneficial effect of enhancing apelin receptor signaling has been proposed.[1]

Recently, 2 groups independently identified a well-conserved gene encoding a peptide named elabela (ELA)[4] or toddler,[5] required for early cardiac development in zebrafish. It is intriguing that the gene (*APELA*) was identified in a region not previously annotated as coding DNA. The *APELA* gene was predicted to express a 54-amino-acid protein comprising a 32-amino-acid mature peptide (ELA-32). Loss of this gene resulted in a rudimentary or no heart in fish embryos, a phenotype similar to loss of the gene *APLNR* encoding the apelin receptor. Both *APELA* and *APLNR* genes are expressed before gastrulation, whereas crucially the established ligand for this receptor, apelin (gene *APLN*), is not present and only expressed later in development. In agreement, deletion of the apelin gene did not produce the same phenotype as deletion of the apelin receptor gene, suggesting the presence of a second ligand such as ELA. In support, ELA was demonstrated to internalize the apelin receptor in vitro, and activation of the apelin signaling pathway was shown to rescue *APELA* mutants. It is interesting to speculate that ELA might be the first in a series of yet uncharacterized developmental signals.[4,5] From these studies the existence of 3 peptides was proposed: ELA-32, ELA-21, and ELA-11 (Figure 1A).

Our aim was to investigate the receptor pharmacology, expression pattern, and in vivo function of ELA peptides in the normal adult cardiovascular system and to seek evidence for alteration in PAH. Using *in silico* molecular modeling and docking, we propose a binding mode of ELA to the apelin receptor that is consistent with competition binding experiments, where the binding affinity of ELA was determined in human heart, a clinically relevant target. We have used cell-based pharmacological assays to show that ELA peptides activated the apelin receptor to inhibit cAMP production and to induce β-arrestin recruitment and receptor internalization. Results from real-time quantitative polymerase chain reaction experiments indicated the presence of *APELA* mRNA in human blood vessels with immunofluorescence staining, confirming the presence of mature ELA peptide localized to the vascular endothelium. ELA peptide was also detectable in human plasma. The acute cardiovascular effects of ELA in rat in vivo included increased cardiac contractility, ejection fraction and cardiac output, and, in addition, vasodilatation. Immunostaining and real-time quantitative polymerase chain reaction showed reduced expression in cardiopulmonary tissues from human PAH patients and 2 rat models of PAH, respectively. Crucially, we have demonstrated that ELA can attenuate the severity of changes in cardiopulmonary function/histology in the monocrotaline (MCT) rat model of PAH in vivo.

METHODS

The online-only Data Supplement Methods provides an expanded description of all experimental protocols. Human tissue samples were obtained with informed consent (Papworth Hospital Research Tissue Bank REC08/H0304/56) and local ethical approval (REC05/Q0104/142). All rodent experiments were performed according to the local ethics committee (University of Cambridge Animal Welfare and Ethical Review Body) and Home Office (UK) guidelines under the 1986 Scientific Procedures Act.

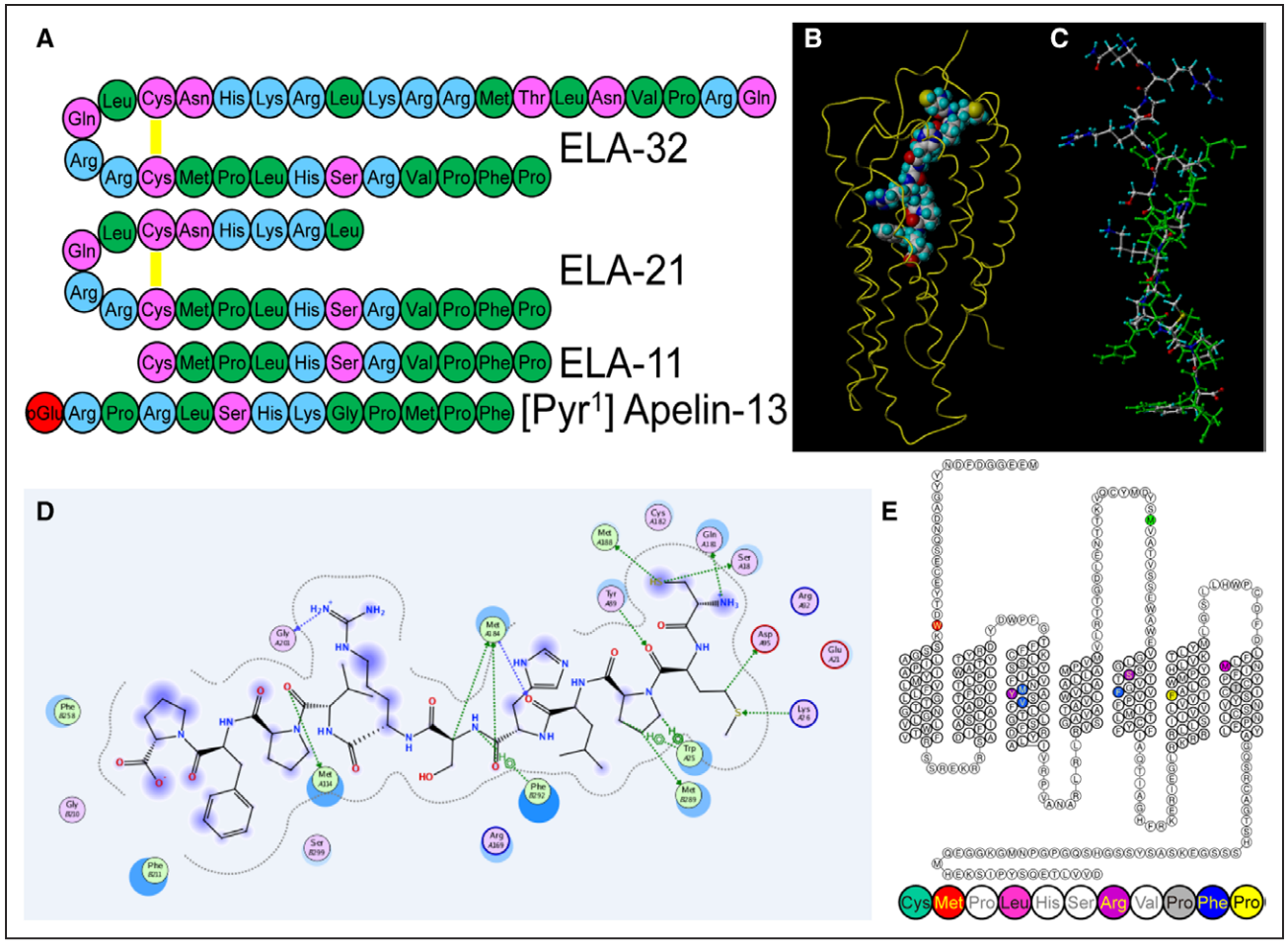

Figure 1. ELA peptides bind to the human apelin receptor.
A, Amino acid sequences of ELA-32, ELA-21, ELA-11, and [Pyr^1]apelin-13. Disulfide bridges are yellow lines, hydrophobic amino acids are shown in green, uncharged polar amino acids in pink, basic amino acids in blue with pyroglutamate in red. **B,** Docking of ELA-11 with the apelin receptor. **C,** Apelin-13 (multicolored atoms) and ELA-11 (green) docking showing overlap in the binding site. **D,** Ligand interaction diagram showing key close contacts between ELA-11 and the apelin receptor model. **E,** Predicted interactions of ELA-11 with the apelin receptor determined by docking analysis. Amino acids in the ELA-11 sequence are color coded to match their predicted sites of interaction on the receptor sequence. ELA indicates Elabela/toddler.

Computational Methods

Docking of ELA-11 and the apelin receptor was conducted using the homology model of apelin and the GOLD docking algorithm as described previously.[6]

Competition Binding

Experiments were conducted in homogenate of human ventricle or Chinese hamster ovary (CHO)-K1 cells expressing the human apelin receptor. Affinity (pK_i) and receptor density (B_{MAX} fmol/mg) for ELA-32, ELA-21, and ELA-11 in human left ventricle (LV) were compared by 1-way analysis of variance (ANOVA), with Tukey multiple comparison. Data (pK_i and B_{MAX}) for ELA-21 were compared between control LV and PAH LV and between control right ventricle (RV) and PAH RV by 2-tailed Student *t* test.

Cell-Based Assays

Inhibition of cAMP accumulation, β-arrestin recruitment, and receptor internalization assays were used to determine values of potency (pD_2 [$-\log_{10}$ EC_{50}]) and maximum response (E_{MAX}). pD_2 values were compared by using 1-way ANOVA with Tukey multiple comparison.

Protein phosphorylation levels for an array of downstream signaling enzymes and levels of secreted angiogenic factors were determined by using pulmonary artery endothelial (PAECs) and smooth muscle cells treated with 0.1% serum, [Pyr^1]apelin-13 or ELA-32 (both 100 nmol/L). Data were analyzed by 1-way ANOVA for matched data with Tukey multiple comparison.

Real-Time Quantitative Polymerase Chain Reaction

RNA extraction, reverse transcription, and real-time quantitative polymerase chain reaction were performed as described in the online-only Data Supplement. For primer sequences, see online-only Data Supplement Table I.

Immunostaining

Immunostaining was performed[7] to localize ELA expression in human normal and PAH tissues using ELA antiserum that cross-reacted with ELA peptides, but not apelin (online-only Data Supplement Figure I), and to assess the effect of ELA-32 treatment on pulmonary vascular remodeling and cardiomyocyte hypertrophy in the MCT rat model as described in the online-only Data Supplement.

Enzyme Immunoassays

Levels of ELA and apelin in healthy human plasma (n=25) were measured by using enzyme immunoassays compared using Student *t* test, and the correlation coefficient (Pearson *r*) was determined.

MRI and Catheterization

The acute cardiac effects of ELA-32 and [Pyr^1]apelin-13 were assessed by MRI and cardiac catheterization. MRI was performed in male Sprague Dawley rats (264±2 g) anesthetized with isoflurane (1.5%–2.5%, inhaled). Peak effects of ELA-32, [Pyr^1]apelin-13, and saline on ejection fraction were expressed as change from baseline and compared by 1-way ANOVA with Dunnett post test.

In a second study, a pressure volume catheter was inserted to monitor LV hemodynamics in male Sprague Dawley rats (257±7 g) anesthetized with isoflurane (1.5% inhaled). Peak effects of ELA-32, [Pyr^1]apelin-13, and saline on LV systolic pressure, cardiac output, stroke volume, contractility (dP/dt_{MAX}), and heart rate were expressed as a change from baseline and compared by 1-way ANOVA with Dunnett post test.[8]

MCT-Induced Rat Model of PAH

Male Sprague Dawley rats (205±2 g) were injected subcutaneously with MCT (60 mg/kg, n=18) or 0.9% saline (n=17) on day 0. MCT- (n=9) or saline (n=9)-exposed animals received daily intraperitoneal injections of ELA-32 (450 μg/kg) with the remainder (MCT, n=9; saline, n=8) receiving saline. On day 21, RV hemodynamics, RV hypertrophy, and pulmonary vascular remodeling were assessed and group data compared by using 1-way ANOVA with Tukey post test. The effect of chronic ELA administration on systemic blood pressure was investigated by LV catheterization in ELA control and saline control animals (n=5 each group) as described above.

Statistical Analyses

Data are expressed as mean±standard error of the mean. Data and statistical analyses were conducted in GraphPad Prism 6. $P \leq 0.05$ was considered statistically significant.

RESULTS

ELA Binds to the Apelin Receptor in Human Normal and PAH Heart

Structural alignment of ELA-11 and apelin-13 docked to the apelin receptor indicated they share a significant hydrophobic binding derived from the presence of the C-terminal hydrophobic moiety in a complimentary hydrophobic pocket of the apelin receptor. However, ELA-11 lacks positively charged residues directly corresponding to the important N-terminal RPRL motif in apelin-13 required for initial recognition of the peptide, although it is interesting to note that there are positively charged amino acids in this region in the longer ELA sequences (Figure 1A). We have recently described a possible pose of apelin-13 interacting with the apelin receptor cavity[6]; given the similarities of the C terminus, we assumed that the pose of this region might be comparable for ELA-11. It has been hypothesized that F10 on ELA-11 may assume a pose similar to F13 on apelin-13,[6] and our model indicated that the binding cavity is large enough to accept the additional C-terminal hydrophobic proline (P11) of ELA-11. Following docking analysis, the pose that consistently showed the best GOLD docking score is shown in Figure 1B. ELA-11 and apelin-13 showed a high degree of overlap in the binding site (Figure 1C). The ELA-11 pose obtained after docking analysis showed a large number of interactions with the apelin receptor (Figure 1D), mainly involving the hydrophobic residues in the N-terminal and C-terminal section of the peptide (Figure 1E) but also including hydrogen bonds.

In human LV ELA-32 (pK_i=9.59±0.08) had significantly ($P \leq 0.0001$) higher affinity than ELA-21 (pK_i=8.52±0.11) and [Pyr^1]apelin-13 (pK_i=8.85±0.04), which were comparable. In contrast, ELA-11 (pK_i=7.85±0.05) had significantly lower affinity than the other peptides ($P \leq 0.01$) (Figure 2A) suggesting that a longer sequence with positively charged residues in the N terminus is required for optimal binding affinity. This is supported by data for the extended peptide ELA-14 that competed for binding in CHO-K1 cells with subnanomolar affinity (pK_i=9.35±0.02), whereas cyclo[1–6]ELA-11 had lower affinity, as expected (pK_i=7.27±0.03).

ELA-21 bound with comparable affinities in RV and LV from human normal and PAH hearts (RV, normal pK_i=8.98±0.04, PAH pK_i=9.30±0.07; LV, normal pK_i=9.31±0.11, PAH pK_i=9.46±0.10) (Figure 2B). In PAH heart in comparison with control, there was a small (≈15%) but significant reduction in apelin receptor density in both LV (PAH 3.42±0.15 fmol/mg, normal 3.96±0.08 fmol/mg; $P \leq 0.05$) and RV (PAH 3.5±0.05 fmol/mg, normal 4.24±0.03 fmol/mg, $P \leq 0.001$).

Receptor Pharmacology of ELA in Vitro

ELA-32, ELA-21, ELA-11, and [Pyr^1]apelin-13 completely inhibited forskolin-induced cAMP production in a concentration-dependent manner (Figure 3A) with subnanomolar potencies (Table). The potency of ELA-11 was comparable to the longer ELA peptides, indicating that this short sequence retains full biological activity in this G-protein–coupled assay.

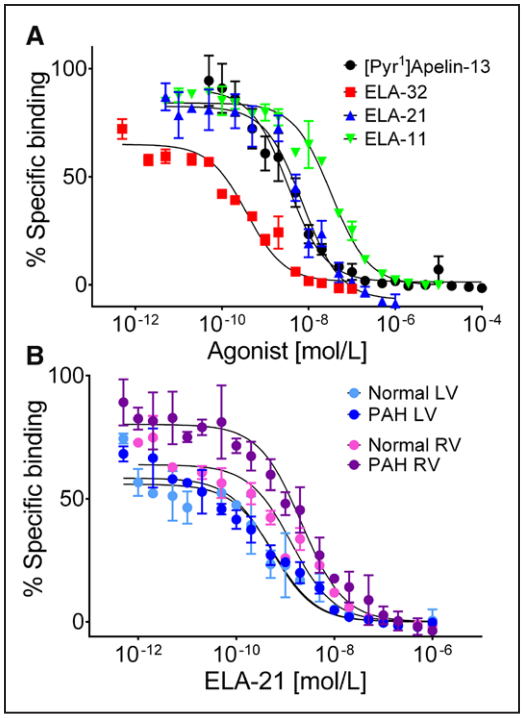

Figure 2. Competition binding curves for ELA peptides in human heart.
A, ELA-32, ELA-21, ELA-11, and [Pyr^1]apelin-13 in human left ventricle. **B**, ELA-21 in normal right ventricle, PAH right ventricle, normal left ventricle, and PAH left ventricle. Values are mean±SEM, n=3. ELA indicates Elabela/toddler; PAH, pulmonary arterial hypertension; and SEM, standard error of the mean.

ELA-32, ELA-21, ELA-11, and [Pyr^1]apelin-13 stimulated β-arrestin recruitment in a concentration-dependent manner (Figure 3B) with similar efficacy. ELA-32 and ELA-21 exhibited comparable pD_2 values and were significantly more potent than ELA-11. A similar rank order of potency was obtained in the internalization assay (Figure 3C), suggesting that a longer sequence is required for optimal activation of the β-arrestin pathway (Table). ML221 (Tocris) antagonized the concentration-response curves to ELA-32 (Figure 3D) and [Pyr^1]apelin-13 (Figure 3E) in the β-arrestin recruitment assay with comparable pA_2 values of 6.87 and 6.91, respectively. ELA-14 (pD_2=10.09±0.12) and cyclo[1–6]ELA-11 (pD_2=9.42±0.32) exhibited subnanomolar potency in the cAMP assay (Figure 3F) similar to the other ELA peptides. In β-arrestin, ELA-14 (pD_2=9.08±0.04) was equipotent with ELA-32 and cyclo[1–6]ELA-11 (pD_2=7.67±0.02) had potency comparable to ELA-11 (Figure 3G).

In control PAECs and control and PAH pulmonary artery smooth muscle cells, apelin and ELA-32 increased levels of ERK1/2 phosphorylation, and in PAECs there was also a significant increase in phosphorylation of endothelial nitric oxide synthase (online-only Data Supplement Figure IIA through IID). Phosphorylation levels of other kinases (online-only Data Supplement Figure III) and levels of secreted angiogenic factors (online-only Data Supplement Figures IV and V) were unaffected.

ELA Is Expressed in Human Cardiovascular Tissues

Expression of *APELA* transcript was observed in all human blood vessels investigated (Figure 4A). With the exception of the aorta, there was a trend for *APELA* expression to be higher in arteries than in veins. Lower levels were detectable in heart and lung (not shown).

Punctate staining of ELA-like immunoreactivity (-LI) and von Willebrand factor-LI were observed in human PAECs but not colocalized to the same intracellular vesicles (Figure 4B). ELA-LI was found in the intima of coronary (Figure 4C) and mammary arteries (Figure 4D), and colocalized with von Willebrand factor. Endothelial ELA-LI was detectable in blood vessels in the heart (Figure 4E) and lung (Figure 4F, online-only Data Supplement Figure VI). No ELA-LI was observed in smooth muscle cells or cardiomyocytes.

ELA and apelin were detectable in healthy human plasma at 0.34±0.03 nmol/L and 0.26±0.03 nmol/L, respectively (Figure 4G), with significantly higher levels of ELA than apelin (P≤0.05). There was a weak, but significant (P≤0.05), positive correlation between ELA and apelin peptide levels (Pearson's r=0.47) (Figure 4H).

Cardiovascular Effects of ELA in Rodents in Vivo

ELA-32 and [Pyr^1]apelin-13 directly strengthened cardiac contractions in vivo, as illustrated in the representative MRI videos (online-only Data Supplement Movies I and II) and snapshots (Figure 5A and 5B). ELA-32 and [Pyr^1]apelin-13 dose-dependently increased LV and RV ejection fractions (Figure 5C and 5D). Low-dose ELA-32 (20 nmol) and [Pyr^1]apelin-13 (50 nmol) increased ejection fraction by 10.3±0.7% (P≤0.0001) and 4.9±1.4% (P>0.05) in LV, respectively, in comparison with saline control (2.0±0.6%) and by 8.0±1.5% (P≤0.001) and 4.4±0.5% (P>0.05) in RV, respectively, in comparison with saline control (1.0±0.8%). High-dose ELA-32 (150 nmol) and [Pyr^1]apelin-13 (650 nmol) significantly increased ejection fraction in LV by 13.5±1.7% (P≤0.05) and 15.8±3.6% (P≤0.01), respectively, in comparison with saline control (1.9±1.0%), and in RV by 9.0±1.8% (P≤0.05) and 8.7±1.0% (P≤0.05), respectively, in comparison with saline control (1.2±1.7%). Effects were short acting and returned to baseline after 10 minutes for the low dose, but were still present at 10 minutes for the high dose. ELA-32 appeared more potent than [Pyr^1]apelin-13, because lower doses of ELA-32 were able

Circulation. 2017;135:1160–1173. DOI: 10.1161/CIRCULATIONAHA.116.023218

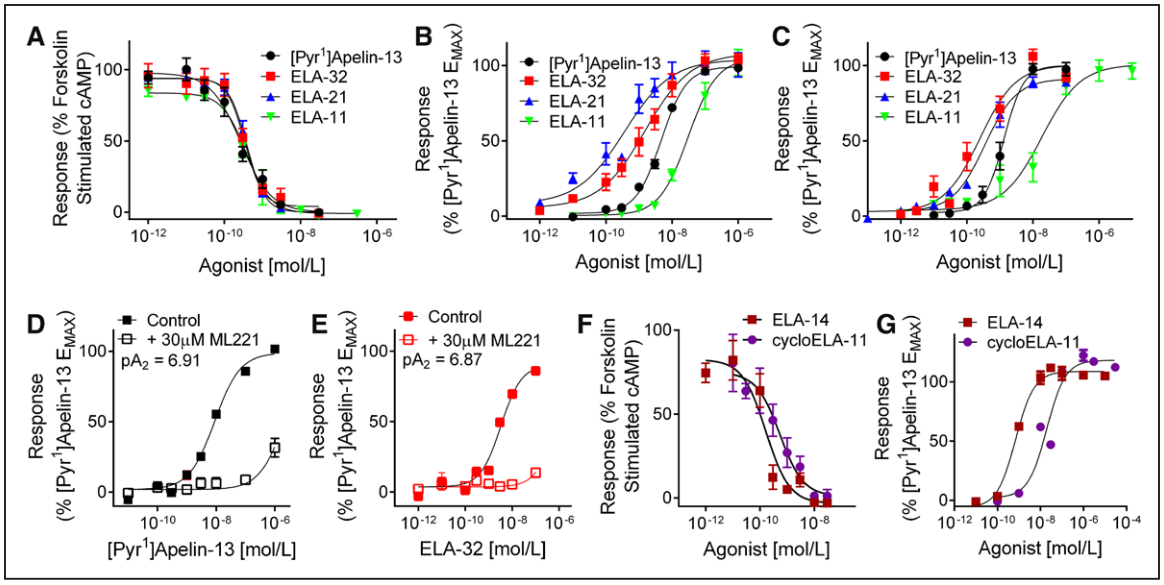

Figure 3. Concentration-response curves in cell-based receptor pharmacology assays.
A, Inhibition of forskolin-induced cAMP accumulation. **B,** Stimulation of β-arrestin recruitment. **C,** Induction of receptor internalization. [Pyr[1]]apelin-13, ELA-32, ELA-21, and ELA-11. Antagonism of [Pyr[1]]apelin-13 (**D**) and ELA-32 (**E**) by 30 μmol/L ML221 in the β-arrestin assay. Concentration-response curves to ELA-14 and cyclic ELA-11 in cAMP (**F**) and β-arrestin (**G**) assays. Values are mean±SEM, n=3 to 5 assays, 2 to 6 replicates per assay. ELA indicates Elabela/toddler; and SEM, standard error of the mean.

to achieve equivalent or more pronounced effects than [Pyr[1]]apelin-13.

In the second rat study, ELA-32 (20 nmol) and [Pyr[1]]apelin-13 (50 nmol) caused a rapid increase in dP/dt_{MAX} of 1217±272 mmHg/s ($P \leq 0.01$) and 493±144 mmHg/s ($P > 0.05$) from baseline, respectively, in comparison with saline control (49±71 mmHg/s). At the higher dose, ELA-32 (150 nmol) and [Pyr[1]]apelin-13 (400 nmol) significantly increased dP/dt_{MAX} by 2825±565 mmHg/s ($P \leq 0.01$) and 3025±680 mmHg/s ($P \leq 0.01$), respectively, in comparison with saline control (142±69 mmHg/s) (Figure 6A). This effect on contractility coincided with a significant increase in cardiac output at both doses of ELA-32 (20 nmol, 3296±370 relative volume units/min (RVU/min), $P \leq 0.0001$; 150 nmol, 4000±826 RVU/min, $P \leq 0.01$) and [Pyr[1]]apelin-13 (50 nmol, 1535±189 RVU/min, $P \leq 0.05$; 400 nmol, 3989±537 RVU/min, $P \leq 0.01$) in comparison with saline control (352±86 RVU/min; 716±215 RVU/min) (Figure 6B). The increase in cardiac output was mostly attributable to an increased stroke volume, because end-systolic volume was reduced. Stroke volume was also significantly increased by ELA-32 (20 nmol, 8.2±0.9 RVU, $P \leq 0.0001$; 150 nmol, 9.1±1.9 RVU, $P \leq 0.01$) and [Pyr[1]]apelin-13 (50 nmol, 3.6±0.5 RVU, $P \leq 0.05$; 400 nmol, 9.2±0.9 RVU, $P \leq 0.001$) in comparison with saline control (0.6±3.4 RVU, 1.6±0.5 RVU) (Figure 6C). A trend toward increased heart rate for both peptides did not reach statistical significance (online-only Data Supplement Figure VII). This effect was followed by a significant dose-dependent reduction in LV systolic pressure by ELA-32 (20 nmol, 14.1±1.6 mmHg, $P \leq 0.0001$; 150 nmol, 17.1±3.2 mmHg, $P \leq 0.01$) and [Pyr[1]]apelin-13 (50 nmol, 8.2±1.1 mmHg, $P \leq 0.01$; 400 nmol, 8.2±3.2 mmHg, $P \leq 0.01$), in comparison with the saline controls (0.6±1.1 mmHg; 1.1±0.3 mmHg) (Fig-

Table. Potency (pD_2) and Efficacy (E_{MAX}) of [Pyr[1]]apelin-13, ELA-32, ELA-21, and ELA-11 in cAMP Inhibition, β-Arrestin Recruitment, and Receptor Internalization Assays

Peptide	cAMP		β-Arrestin		Internalization	
	pD_2	E_{MAX}, %	pD_2	E_{MAX}, %	pD_2	E_{MAX}, %
[Pyr[1]]apelin-13	9.74±0.11	100±1	8.10±0.12	100±2	8.87±0.25	100±2
ELA-32	9.49±0.07	101±1	9.05±0.32††	104±4	9.66±0.36†	102±4
ELA-21	9.43±0.16	101±1	9.88±0.29**†††	102±1	9.55±0.08	96±2
ELA-11	9.13±0.21	100±1	7.44±0.18	107±6	8.13±0.56	105±1

Values are mean±standard error of the mean, n=3–5 assays, 2–6 replicates per assay. ELA indicates Elabela/toddler.
**$P \leq 0.01$, significantly different from [Pyr[1]]apelin-13.
†$P \leq 0.05$, ††$P \leq 0.01$, †††$P \leq 0.001$, significantly different from ELA-11.

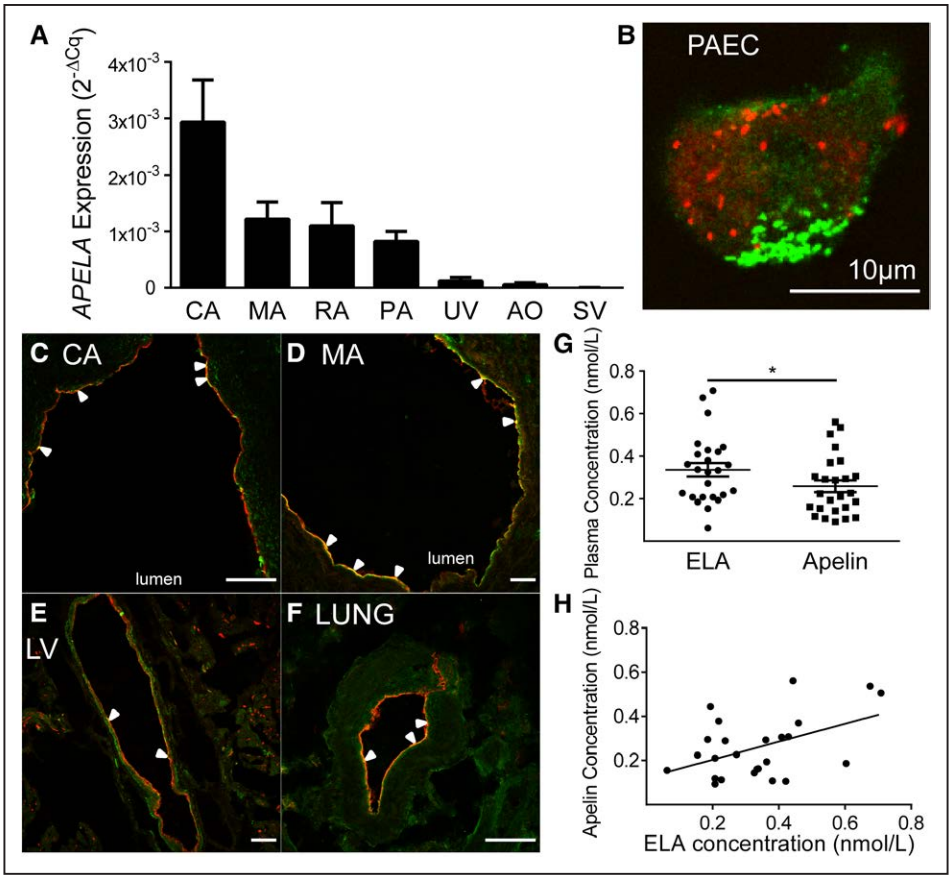

Figure 4. Expression of *APELA* transcript and ELA peptide in human cardiovascular tissues.
A, Expression of *APELA* mRNA in human blood vessels determined by RT-qPCR. **B** through **F**, Representative overlay confocal photomicrographs of immunofluorescence staining of human pulmonary artery endothelial cell (PAEC) (**B**) and human cardiovascular tissue (**C** through **F**). Photomicrographs show ELA-like immunoreactivity in green and the endothelial marker vWF in red. If not indicated, scale bars=75 μm. CA, coronary artery (n=11); MA, mammary artery (n=6); RA, radial artery (n=9); PA, pulmonary artery (n=4); UV, umbilical vein (n=6); AO, aorta (n-6); SV, saphenous vein (n=8); LV, left ventricle (n=8); lung (n=6). **G,** Levels of ELA and apelin in human plasma (n=25). **H,** Correlation between plasma concentrations of ELA and apelin. **P*<0.05 in comparison with ELA. ELA indicates Elabela/toddler; RT-qPCR, real-time quantitative polymerase chain reaction; and vWF, von Willebrand factor.

ure 6D). A third, higher dose of [Pyr[1]]apelin-13 (1300 nmol) did not show further increase in any response. To confirm the contribution of systemic vasodilatation to the reduction in LV systolic pressure, ELA-32 and [Pyr[1]]apelin-13 were each administered to 1 animal in which the catheter was placed in the carotid artery and both elicited a comparable reduction in systolic and diastolic blood pressure (not shown). Consistent with the MRI experiment, the cardiovascular effects of ELA-32 and [Pyr[1]]apelin-13 were short acting, returning to baseline within 10 to 20 minutes. Moreover, the response to ELA-32 appeared to be greater than the same dose of [Pyr[1]]apelin-13.

Downregulation of ELA Expression in Human PAH and Rodent Models of PAH

The number of ELA-positive and ELA-negative blood vessels in control human lung sections was 84±3 versus 16±3, in comparison with 58±5 versus 42±5 in PAH lung (Fisher exact test, $P \leq 0.0001$; Figure 7A). In comparison with controls, the proportion of ELA-positive vessels was significantly reduced, whereas the proportion of ELA-negative vessels was significantly increased in PAH (online-only Data Supplement Figure VIII).

Expression of *APELA* mRNA in human PAH lung was significantly ($P \leq 0.01$) reduced in comparison with healthy lung (Figure 7B). *Apela* mRNA level in RV was significantly reduced in both Sugen/hypoxia ($P \leq 0.05$) and MCT rats ($P \leq 0.01$) in comparison with controls (Figure 7C and 7D). It is interesting to note that *Aplnr* mRNA in RV was also significantly lower in the MCT rats than in controls ($P \leq 0.01$) (Figure 7E), and there was a trend (not significant, $P=0.14$) for reduced expression of *Apln* mRNA in these animals (Figure 7F).

Attenuation of MCT-Induced PAH by ELA

MCT administration elevated RV systolic pressure (81.3±6.0 mm Hg, $P \leq 0.0001$) in comparison with saline controls (27.4±0.6 mm Hg). ELA-32 treatment in

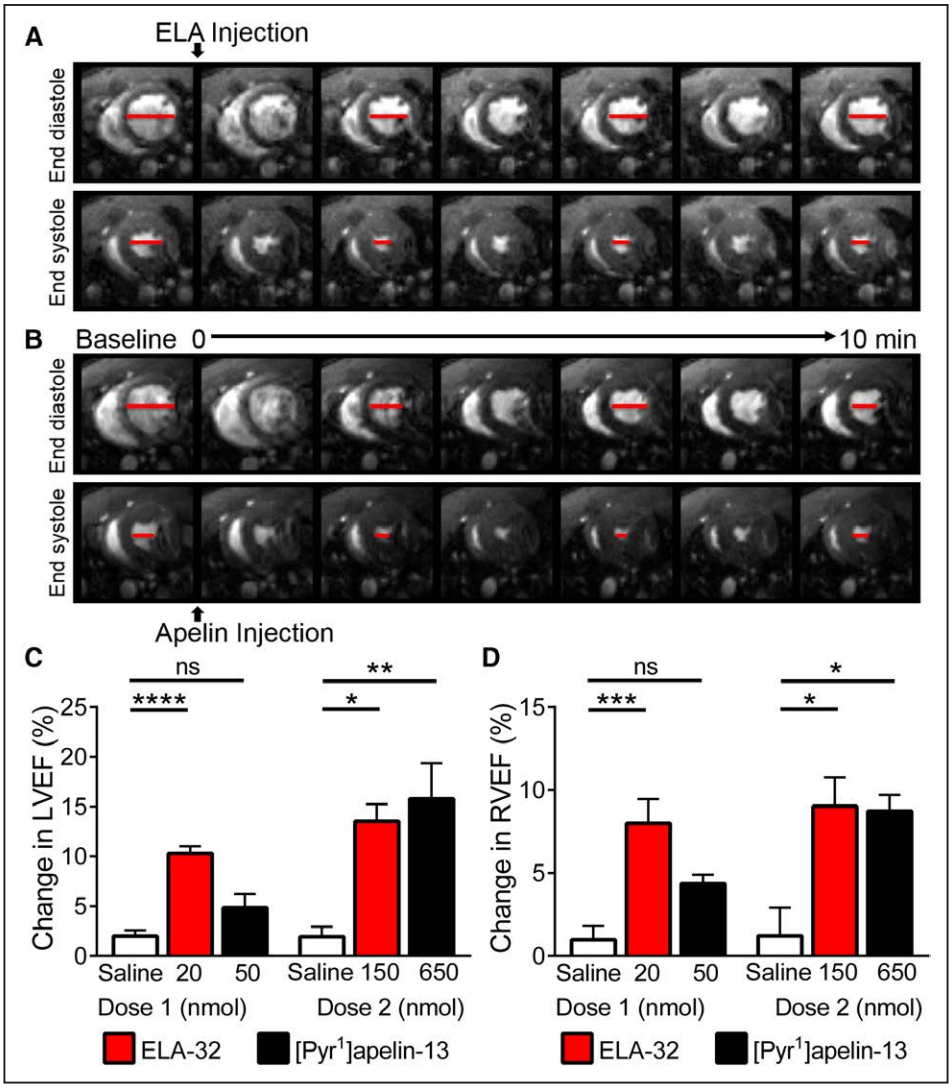

Figure 5. Cardiac effects of ELA and apelin in vivo by MRI in the rat.
Representative snapshots of midventricular transverse sections of the heart at end-diastolic and end-systolic points during the 10-minute MRI scan showing the effects of ELA-32 (150 nmol) (**A**) and [Pyr^1]apelin-13 (650 nmol) (**B**). Red bars are drawn to show the approximate diameter of the left ventricle. Dose-dependent increase in left (**C**) and right (**D**) ventricular ejection fraction of the heart in response to ELA-32 (red bars, 20 and 150 nmol, n=8) and [Pyr^1]apelin-13 (black bars, 50 and 650 nmol, n=5). **P*<0.05. ***P*<0.01. ****P*<0.001. *****P*<0.0001 in comparison with saline control (n=6). ELA indicates Elabela/toddler; LVEF, left ventricular ejection fraction; ns, not significantly different from saline control; and RVEF, right ventricular ejection fraction.

MCT rats attenuated RV systolic pressure (52.5±1.9 mm Hg, *P*≤0.0001 versus MCT group), but this was still significantly higher than control RV systolic pressure (*P*≤0.0001 versus saline group) (Figure 8A). Similarly, in comparison with the saline controls (Fulton index=0.21±0.01), RV hypertrophy was observed in MCT rats (0.46±0.02, *P*≤0.0001) that was significantly attenuated by ELA-32 administration (0.32±0.02, *P*≤0.0001 versus MCT group, *P*≤0.05 versus saline group) (Figure 8B). MCT increased the percentage of fully muscularized vessels (MCT 28±2% versus saline 8±1%, *P*≤0.0001) and arteriolar wall thickness (MCT 26±1% versus saline 10±1%, *P*≤0.0001), and this was significantly lessened by ELA-32 (muscularization, 19±2%, *P*≤0.01 versus MCT; wall thickness, 16±1% versus MCT, *P*≤0.0001) (Figure 8C through 8L). MCT exposure resulted in significant RV hypertrophy indicated by an increase in cardiomyocyte area (wheat germ agglutinin staining; MCT 315±9 μm^2 versus saline 212±11 μm^2, *P*≤0.0001), a reduction in cardiomyocyte number/area (MCT 59±2 versus saline 91±1, *P*≤0.0001) and an increase in GATA4-positive nuclei/area (MCT 44±2 versus saline 30±1, *P*≤0.0001). There was a significant improvement in these indices following ELA-32 treatment (cardiomyocyte area 228±9 μm^2, *P*≤0.0001 in comparison with MCT alone; cardiomyocyte number/area 66±2; GATA4 positive nuclei/area 38±1 (both *P*≤0.05 in comparison with MCT alone) (Fig-

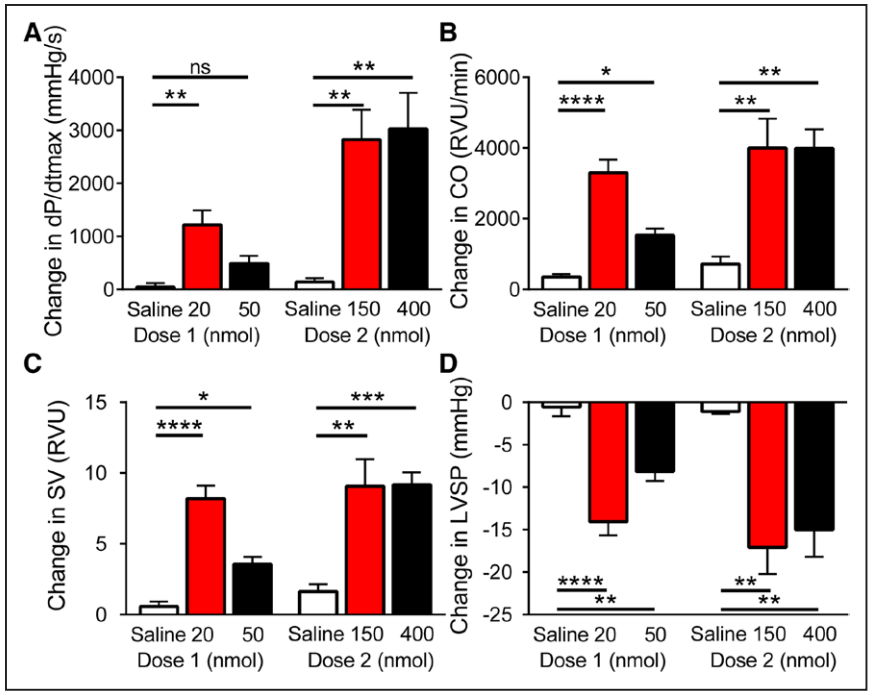

Figure 6. The in vivo effects of ELA-32 and [Pyr¹]apelin-13 on the left ventricle of rat heart measured by catheterization. Compared to saline controls (open bars, n=6), ELA-32 (red bars, n=10), and [Pyr¹]apelin-13 (black bars, n=8) caused a significant change in cardiac contractility (dP/dt_{MAX}) (**A**), cardiac output (CO) (**B**), stroke volume (SV) (**C**), and LV systolic pressure (LVSP) (**D**). **P*<0.05. ***P*<0.01. ****P*<0.001. *****P*<0.0001 in comparison with saline control. ELA indicates Elabela/toddler; LV, left ventricular; RVU, relative volume unit; and ns, not significantly different from saline control.

ure 8M through 8O, online-only Data Supplement Figure IX). ELA-32 had no significant effect in comparison with saline control on any hemodynamic or histological parameter in this study and, in particular, did not cause systemic hypotension following chronic administration (online-only Data Supplement Figure X). There was some evidence of improved survival in the MCT-ELA group in comparison with MCT alone, because in the MCT group 1 rat died (day 18) and 3 died under isoflurane, whereas only 1 MCT-ELA rat died (day 20). Plasma levels of the vasoactive peptides angiotensin-II and BNP-32 were unaltered by ELA-32 treatment (online-only Data Supplement Figure XI).

DISCUSSION

This study provides a comprehensive characterization of ELA, originally reported as a regulator of zebrafish cardiac development, in the adult mammalian cardiovascular system. We report for the first time ELA peptides binding to the native human apelin receptor, ELA expression in human blood vessels, attenuation of cardiac dysfunction, cardiac and pulmonary arterial remodeling, and peptide and receptor mRNA expression in human PAH and rodent models of PAH, in addition to more fully characterizing the cardiovascular profile of ELA in comparison with apelin.

Receptor Binding and Downstream Signaling

Using cells overexpressing the receptor and ELA conjugated to alkaline phosphatase, Chng et al[4] were the first to suggest that ELA could bind to the human apelin receptor. In this study, we initially used molecular dynamic simulation based on homology models of the apelin receptor to create a receptor template into which ELA could be reliably docked. Despite the lack of obvious sequence similarity, ELA-11 docked within the binding pocket occupied by apelin-13. We subsequently confirmed this in radioligand competition assays using [^{125}I] apelin-13 to demonstrate direct binding of all 3 ELA peptides to the apelin receptor in human cardiac tissue. Our data from both heart and CHO cells revealed that ELA-32, ELA-21, and ELA-14 bound to the human receptor with subnanomolar affinity, whereas the linear and cyclo[1–6] ELA-11 displayed a 100-fold drop in affinity, consistent with a recent report using HEK293 cells expressing the apelin receptor.[9] This confirms the importance of positively charged amino acids (which interact via hydrogen bonding with the apelin receptor in our model system) in the longer ELA peptides corresponding to the RPRL motif in apelin-13 that we have previously identified as critical for receptor-binding affinity.[10] Similar or lower affinities for ELA conjugated to alkaline phosphatase have been reported in CHO cells expressing apelin receptor (K_d=0.51 nmol/L[11]) and for ELA-32 in isolated rat cardiomyocytes (K_i=38.2 nmol/L[12]). Therefore, although a recent report from the codiscoverers of ELA suggested an unidentified cell surface receptor rather than the apelin receptor is responsible for mediating the effects of ELA in human embryonic stem cells,[13] our data clearly confirm that in the adult cardiovascular system ELA is a ligand for the apelin receptor.

Next, ELA was tested for its ability to activate G-protein signaling using a cAMP inhibition assay, because the apelin receptor is known to couple via G_i. ELA-32, ELA-21, and ELA-11 were full agonists in this assay with comparable potency to [Pyr¹]apelin-13 in the subnanomolar

Circulation. 2017;135:1160–1173. DOI: 10.1161/CIRCULATIONAHA.116.023218

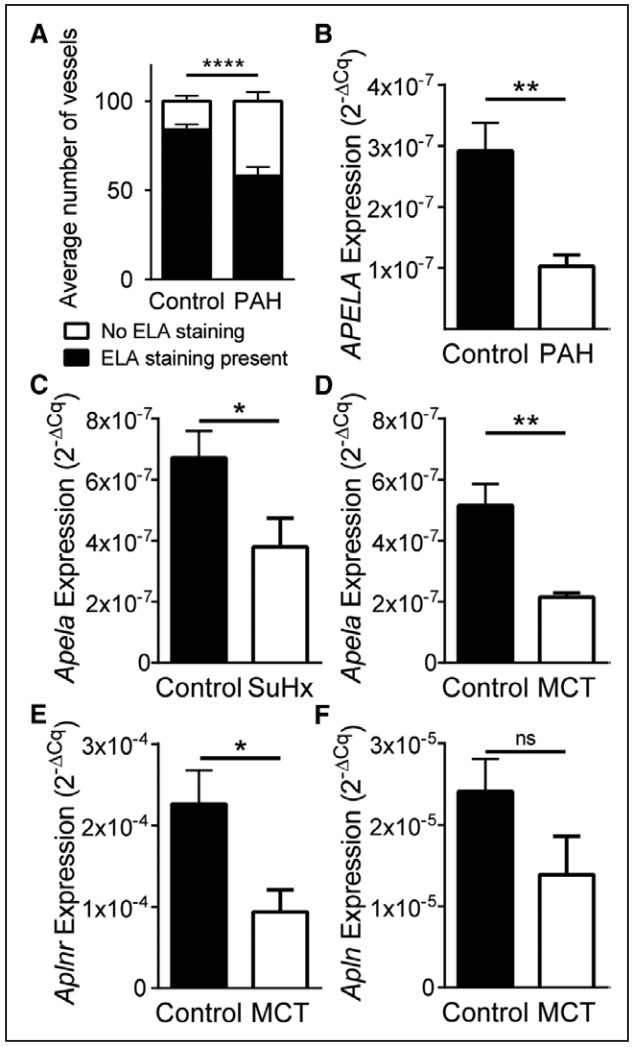

Figure 7. Altered levels of ELA expression in PAH. **A,** Number of blood vessels positive and negative for ELA staining in control (n=4) and PAH (n=4) human lung sections (****$P \leq 0.0001$). **B,** *APELA* downregulation in human PAH (n=4) in comparison with normal (n=4) lung (**$P \leq 0.01$). *Apela,* mRNA downregulation in the right ventricle of Sugen/hypoxia (n=6) (**C**) and MCT exposed (n=5) (**D**) rats (*$P \leq 0.05$, **$P \leq 0.01$, respectively, in comparison with saline (n=7 and 5, respectively). *Aplnr* (**E**) and *Apln* mRNA (**F**) expression in right ventricle of saline (n=5) and MCT exposed (n=5) rats (*$P \leq 0.05$, in comparison with saline. ELA indicates Elabela/toddler; MCT, monocrotaline; ns, not significantly different from saline control; and PAH, pulmonary arterial hypertension.

range, consistent with their high binding affinities. It is interesting to note that ELA-11 and cyclo[1–6]ELA-11 were not different from the longer forms in terms of potency and efficacy in blocking cAMP accumulation, suggesting that the 11-mer was sufficient for effective G_i-protein signaling via the apelin receptor. ELA-14, consistent with our high-affinity binding data, has also been reported to activate G-protein–dependent and –independent pathways with comparable potency to ELA-32,[9] and our data confirm this. Data for ELA-32 have been reported by 2 other groups with EC_{50} values in the subnanomolar[11] to nanomolar[14] range and ELA-mediated inhibition of cAMP production confirmed as pertussis toxin sensitive.[11]

As expected for agonist activation of most G-protein–coupled receptors, apelin binding also triggered recruitment of β-arrestin leading to receptor internalization and β-arrestin–dependent signaling.[15] Our data revealed that, in contrast to their equivalent potency in the G-protein pathway, ELA-32, ELA-21, and ELA-14 were more potent than ELA-11, cyclo[1–6]ELA-11, and [Pyr^1]apelin-13 in the β-arrestin assays. These data are interesting because they provide additional evidence that extended N-terminal sequences of ELA and apelin peptides are more effective in stimulating β-arrestin–mediated cellular events as previously reported for apelin-17 in comparison with [Pyr^1]apelin-13 in cAMP and internalization assays using the expressed rat receptor.[16] Our data expand on initial studies that demonstrated internalization of enhanced green fluorescent protein–tagged apelin receptors in zebrafish embryos by exogenous *APELA* mRNA and ELA-21 peptide[5] and ELA-32–induced internalization of green fluorescent protein–tagged human apelin receptor overexpressed in HEK293 cells.[14] The nonpeptide small-molecule antagonist ML221 blocked responses to ELA-32 and [Pyr^1]apelin-13 in the β-arrestin assay with the same affinity, providing additional evidence that the 2 ligands bind to the same or overlapping sites on the receptor. It is important to note that for drug discovery and therapeutic intervention, these data confirm that apelin receptor antagonists can be designed that will block all apelin signaling irrespective of the endogenous ligand. We conclude from our cell-based assays that the truncated form, ELA-11, preferentially activates G-protein signaling and may represent an endogenous G-protein–biased apelin receptor ligand. How the different apelin and ELA peptides are integrated in normal apelin receptor physiology and how these may contribute to disease progression remain to be unraveled.

ELA Expression in the Human Cardiovascular System

Having established receptor binding and activation by ELA peptides in vitro, we addressed the question of endogenous expression of ELA in relevant human tissues. To date, *APELA* mRNA expression has been reported in human embryonic stem cells,[4,14] induced pluripotent stem cells,[14] kidney[4,14] and prostate,[4] and rat kidney[11] with ELA peptide expression only reported in human embryonic stem cells.[4] Our study is the first report of *APELA* transcript and ELA in human blood vessels suggesting that *APELA* is translated into a peptide in the vasculature. Expression was identified in both large- and small-diameter vessels; for example, in heart, ELA localized to both epicardial and intramyocardial blood vessels. Specifically, ELA peptide expression was re-

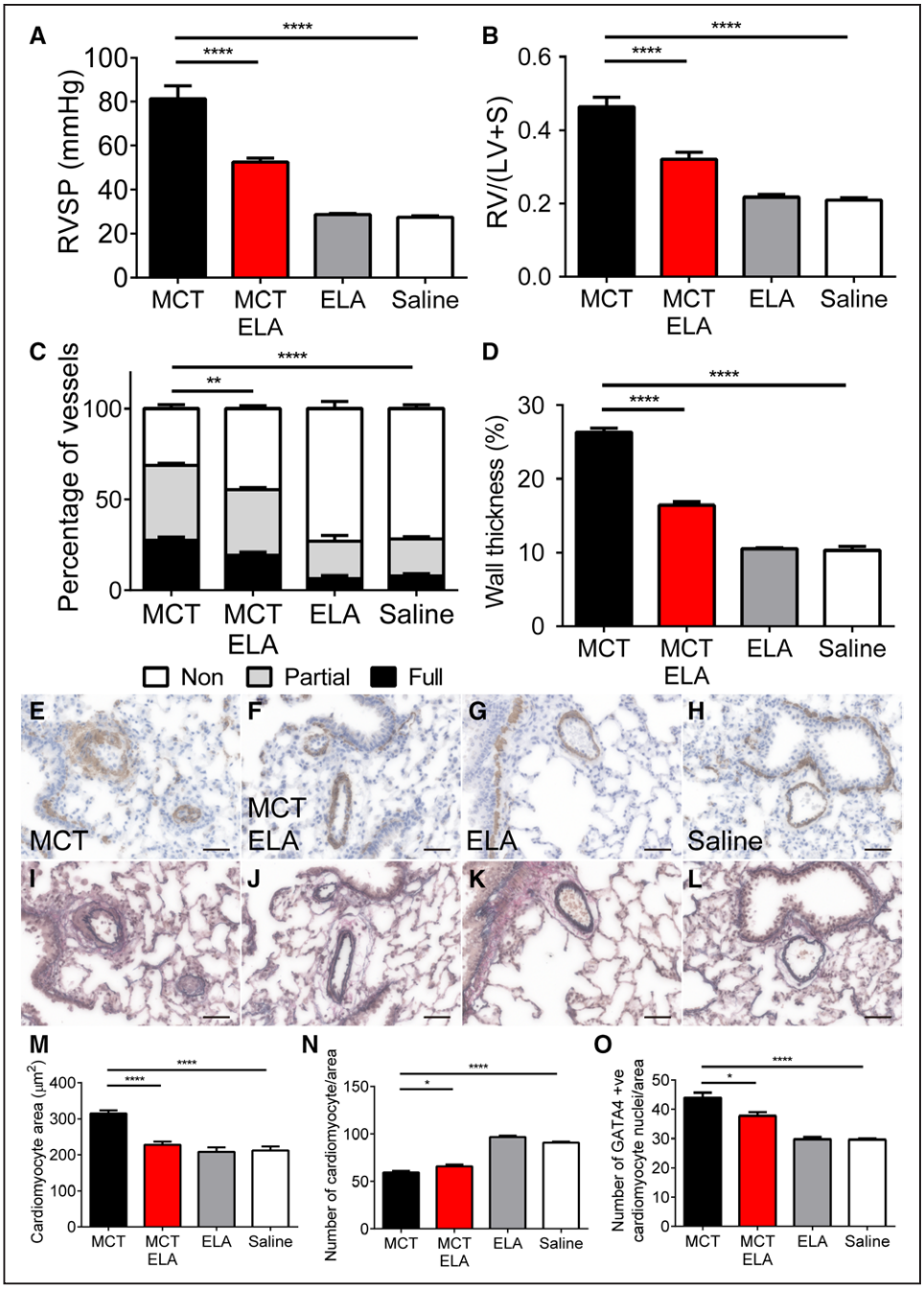

Figure 8. Attenuation of MCT-induced PAH by ELA-32 in rats.
MCT exposure (black bar, n=9) caused an increase in right ventricular systolic pressure (RVSP) (**A**) and right ventricular hypertrophy (**B**) measured as RV/(LV+S) (Fulton index) (both ****$P \leq 0.0001$) in comparison with saline control (open bars, n=8). ELA-32 administration (red bars, n=9) significantly reduced MCT-induced RVSP and hypertrophy (****$P \leq 0.0001$ and ****$P \leq 0.0001$, respectively). ELA-32 alone (gray bars, n=9) had no effect and was not different from saline control (open bars, n=8). In tissues from these animals, MCT increased the proportion of fully muscularized vessels in rat lung (**C**) and wall thickness of larger pulmonary arterioles (**D**) in comparison with saline (both ****$P \leq 0.0001$), and these changes were attenuated by ELA-32 (**$P \leq 0.01$ and ****$P \leq 0.0001$, respectively). Immunohistological visualization of remodeling of pulmonary arterioles using α-smooth muscle actin (brown, **E** through **H**) and van Giesen stain (**I** through **L**) in sections of lung from MCT (**E**, **I**), MCT-ELA (**F**, **J**), ELA alone (**G**, **K**), and saline control rats (**H**, **L**) (scale bars=75μm). MCT-induced RV hypertrophy was indicated by an increase in cardiomyocyte area indicated by WGA staining (**M**), a reduction in cardiomyocyte number/area (**N**), and an increase in GATA4-positive nuclei/area compared to saline control (**O**) (****$P \leq 0.0001$) with a significant improvement in these indices following ELA-32 treatment (*$P \leq 0.05$, **** $P \leq 0.0001$, in comparison with MCT alone). ELA-32 alone had no effect on any parameter. ELA indicates Elabela/toddler; MCT, monocrotaline; LV, left ventricle; ns, not significantly different from saline control; PAH, pulmonary arterial hypertension; RV, right ventricle; and WGA, wheat germ agglutinin.

stricted to the vascular endothelium with no significant localization to vascular smooth muscle or cardiomyocytes. We have previously reported the localization of the apelin receptor to the vascular endothelium, the underlying smooth muscle/cardiomyocytes,[17] raising the possibility that ELA may signal in an autocrine/paracrine manner. We have also localized apelin to the vascular and endocardial endothelium,[7] and therefore an overlapping distribution of the 2 peptides is apparent. The significance of 2 peptides and 1 receptor will need to be addressed; however, in development this is resolved by temporal differences in the expression of each peptide. The expression of *APELA* appeared to be higher in arterial than in venous tissue, with the exception of the aorta. The implication of this trend is not clear. The presence of ELA peptide in the heart was consistent with previous reports on zebrafish, where ELA is critical in cardiac development,[4,5] and Perjés et al[12] recently reported *APELA* mRNA expression in endothelial cells in mouse heart. Staining of cultured primary human endothelial cells verified the presence of ELA peptide in this cell type. It is interesting to note that ELA did not colocalize with Weibel-Palade bodies,[18] suggesting that ELA is produced via a constitutive synthetic pathway rather than via regulated/inducible release. This subcellular spatial localization is also observed with apelin.[17]

Apelin levels have been measured in human plasma by enzyme-linked immunosorbent assay.[19] We therefore used a similar assay to detect ELA peptides. Both ELA and apelin were detectable in human plasma at subnanomolar levels, more indicative of peptides acting as locally released autocrine/paracrine mediators than as circulating hormones. Although we observed a correlation between plasma concentrations of ELA and apelin, the relatively narrow age range of our samples did not allow a more detailed correlation between ELA concentration and, for example, age, sex, or body mass index.

Cardiovascular Effect of ELA in Rodents in Vivo

We next tested if ELA modulates cardiovascular functions in vivo. In heart, apelin is reportedly the most potent inotrope in vitro[3,20] via protein kinase C and extracellular signal–regulated kinases 1/2.[21] Consistent with this are data from in vivo studies in rodents and humans. In anesthetized rats, apelin-16 increased dP/dt_{MAX}[22] and [Pyr^1]apelin-13 increased cardiac output and reduced blood pressure.[6] In anesthetized mice, intraperitoneal injection of [Pyr^1]apelin-13 reduced LV end-diastolic area and increased heart rate, observed using MRI, whereas hemodynamics measurement by catheterization showed an increased preload recruitable stroke work (a measure of intrinsic contractility) and reduced LV end-systolic pressure.[23] In human volunteers, intracoronary bolus administration of apelin-36 increased dP/dt_{MAX}, and an intravenous infusion of apelin-36 or [Pyr^1]apelin-13 increased heart rate and cardiac output.[24]

We have used a combination of MRI and invasive catheterization to characterize the cardiac effects of ELA in comparison with apelin. ELA-32 and [Pyr^1]apelin-13 were positive inotropes in the LV, increasing dP/dt_{MAX} consistent with the previous reports for apelin[22,24] and an initial report of increased fractional shortening by ELA-32.[9] In addition, ELA-32 and [Pyr^1]apelin-13 increased cardiac output, owing to increased stroke volume and possibly increased heart rate. We also observed for ELA-32 the previously reported apelin-induced reduction in LV end-diastolic area,[23] resulting in an increased ejection fraction. We could not detect obvious qualitative differences in the cardiac actions of ELA-32 and [Pyr^1]apelin-13, but Perjés et al[12] reported that the inotropic effect of ELA-32 in vitro in the Langendorff perfused rat heart was dependent on extracellular signal–regulated kinases 1/2 but not on protein kinase C as seen for apelin.

We detected an ELA-32– and [Pyr^1]apelin-13–induced drop in LV systolic pressure. This is likely a consequence of reduced afterload resulting from peripheral vasodilatation, a known effect of apelin.[3,6] To confirm systemic vasodilation, ELA-32 and [Pyr^1]apelin-13 were administered with the catheter placed in the right carotid artery, and both peptides caused a drop in blood pressure in agreement with Murza et al[9]. These in vivo data are consistent with recent in vitro studies suggesting that ELA has a vasodilatory effect in adult rat coronary arteries[12] and caused relaxation of preconstricted mouse aortic rings[14] in a reported nitric oxide–independent and partially endothelium-independent manner. Overall, we observed that lower doses of ELA-32 were required to achieve equivalent or more pronounced effects than [Pyr^1]apelin-13. This is consistent with the ≈5-fold higher receptor affinity we determined for ELA-32 in comparison with [Pyr^1]apelin-13 in human heart.

Reduced ELA Expression in Human PAH and Rodent Models and Attenuation of MCT-Induced PAH by Exogenous ELA in Rats

Last, we addressed the question of the possible alteration in ELA expression in PAH, where apelin expression is known to be reduced, contributing to disease pathogenesis. Apelin levels are downregulated in plasma or serum[19,25] in PAECs[26] and pulmonary microvascular endothelial cells[27] from PAH patients and in RV of MCT-exposed rat.[28] The expression of the apelin receptor was also reduced in RV of MCT rats.[28] We have now shown for the first time that ELA is similarly reduced in pulmonary vessels of PAH patients and in the RV from 2 rodent models of PAH. In particular, ELA staining was examined in small pulmonary blood vessels that are critical to the pathogenesis of PAH, because they undergo vascular remodeling leading to increased vascular resistance and,

consequently, the RV undergoes hypertrophy. We observed a reduction in *Apela* expression in RV of Sugen/hypoxia and MCT-exposed rats and also of *Aplnr* with a trend to reduction in *Apln* in the MCT animals. This is consistent with a downregulation of all components of the ELA/apelin/apelin receptor pathway in the RV in PAH. It is important to note that, although reduced, *Aplnr* mRNA was still present in the RV, making the receptor amenable for therapeutic manipulation with a goal to replace the downregulated ELA or apelin peptides. We confirmed this in human heart where the apelin receptor density in PAH in comparison with normal RV and LV was only reduced by ≈15%. There has been 1 study reporting increased *Apela* and *Aplnr* mRNA expression in LV of a mouse model of myocardial infarction,[12] but we did not observe this for the receptor in LV from human PAH heart. Last, we have shown that, as reported for apelin,[28] administration of ELA-32 attenuated the remodeling of the pulmonary vasculature and hypertrophy of RV cardiomyocytes. This resulted in blunting of the increased RV systolic pressure and hypertrophy induced by MCT in this rat model of PAH.

In conclusion, our study confirms the direct receptor binding of ELA to the apelin receptor in human heart, and provides more details on the docking of this ligand within the receptor using molecular modeling. Using cell-based assays, we compared ELA-32, ELA-21, and ELA-11 with [Pyr^1]apelin-13 and found them to be agonists in G-protein–dependent and –independent pathways. Our data also demonstrated the widespread presence of *APELA* mRNA and ELA peptide in adult human cardiovascular tissues and localized the peptide specifically to the endothelium. Furthermore, we demonstrated in vivo that ELA increases cardiac contractility and cardiac output and causes vasodilatation. These results show that ELA is an endogenous agonist of the human apelin receptor and exhibits a cardiovascular profile comparable to that of apelin. The relative importance of the 2 peptides to normal apelin receptor function needs to be explored. However, the downregulation of ELA expression in PAH and the beneficial effect of ELA administration on cardiac function and cardiopulmonary remodeling in the MCT rat model of PAH, consistent with that of apelin, supports the potential exploitation of the apelin receptor as a therapeutic target at least in this disease.

ACKNOWLEDGMENTS

The authors thank Keith Siew for technical advice and discussion, the theater and consultant staff of Papworth hospital for tissue collection, and Dr Benjamin Garfield for rat tissues.

SOURCES OF FUNDING

This work was supported by the Wellcome Trust 107715/Z/15/Z and Program in Metabolic and Cardiovascular Disease 096822/Z/11/Z, Medical Research Council MC_PC_14116, British Heart Foundation PS/02/001, PG/05/127/19872, FS/14/59/31282, and, in part, by the National Institute for Health Research Cambridge Biomedical Research Center and the Pulmonary Hypertension Association UK.

DISCLOSURES

None.

AFFILIATIONS

From Experimental Medicine and Immunotherapeutics, University of Cambridge, Centre for Clinical Investigation, Addenbrooke's Hospital, UK (P.Y., C.R., R.E.K., J.J.M., A.P.D.); Wolfson Brain Imaging Centre, Department of Clinical Neuroscience, University of Cambridge, UK (G.B., S.J.S., T.A.C.); Department of Pathology, Papworth Hospital, Papworth Everard, Cambridge, UK (M.S.); Centre for Molecular Informatics, Department of Chemistry, University of Cambridge, UK (R.T., R.C.G.); Department of Medicine, University of Cambridge, Addenbrooke's Hospital, UK (P.D.U., A.C., N.W.M.); and Biomolecular Medicine, Department of Surgery and Cancer, Imperial College, London, UK (R.C.G.).

FOOTNOTES

Received April 27, 2016; accepted January 17, 2017.

The online-only Data Supplement is available with this article at http://circ.ahajournals.org/lookup/suppl/doi:10.1161/CIRCULATIONAHA.116.023218/-/DC1.

Circulation is available at http://circ.ahajournals.org.

REFERENCES

1. Yang P, Maguire JJ, Davenport AP. Apelin, Elabela/Toddler, and biased agonists as novel therapeutic agents in the cardiovascular system. *Trends Pharmacol Sci*. 2015;36:560–567. doi: 10.1016/j.tips.2015.06.002.
2. Kang Y, Kim J, Anderson JP, Wu J, Gleim SR, Kundu RK, McLean DL, Kim JD, Park H, Jin SW, Hwa J, Quertermous T, Chun HJ. Apelin-APJ signaling is a critical regulator of endothelial MEF2 activation in cardiovascular development. *Circ Res*. 2013;113:22–31. doi: 10.1161/CIRCRESAHA.113.301324.
3. Maguire JJ, Kleinz MJ, Pitkin SL, Davenport AP. [Pyr1]apelin-13 identified as the predominant apelin isoform in the human heart: vasoactive mechanisms and inotropic action in disease. *Hypertension*. 2009;54:598–604. doi: 10.1161/HYPERTENSIONAHA.109.134619.
4. Chng SC, Ho L, Tian J, Reversade B. ELABELA: a hormone essential for heart development signals via the apelin receptor. *Dev Cell*. 2013;27:672–680. doi: 10.1016/j.devcel.2013.11.002.
5. Pauli A, Norris ML, Valen E, Chew GL, Gagnon JA, Zimmerman S, Mitchell A, Ma J, Dubrulle J, Reyon D, Tsai SQ, Joung JK, Saghatelian A, Schier AF. Toddler: an embryonic signal that promotes cell movement via Apelin receptors. *Science*. 2014;343:1248636. doi: 10.1126/science.1248636.

6. Brame AL, Maguire JJ, Yang P, Dyson A, Torella R, Cheriyan J, Singer M, Glen RC, Wilkinson IB, Davenport AP. Design, characterization, and first-in-human study of the vascular actions of a novel biased apelin receptor agonist. *Hypertension*. 2015;65:834–840. doi: 10.1161/HYPERTENSIONAHA.114.05099.
7. Kleinz MJ, Davenport AP. Immunocytochemical localization of the endogenous vasoactive peptide apelin to human vascular and endocardial endothelial cells. *Regul Pept*. 2004;118:119–125. doi: 10.1016/j.regpep.2003.11.002.
8. Read C, Fitzpatrick CM, Yang P, Kuc RE, Maguire JJ, Glen RC, Foster RE, Davenport AP. Cardiac action of the first G protein biased small molecule apelin agonist. *Biochem Pharmacol*. 2016;116:63–72. doi: 10.1016/j.bcp.2016.07.018.
9. Murza A, Sainsily X, Coquerel D, Côté J, Marx P, Besserer-Offroy É, Longpré JM, Lainé J, Reversade B, Salvail D, Leduc R, Dumaine R, Lesur O, Auger-Messier M, Sarret P, Marsault É. Discovery and structure-activity relationship of a bioactive fragment of ELABELA that modulates vascular and cardiac functions. *J Med Chem*. 2016;59:2962–2972. doi: 10.1021/acs.jmedchem.5b01549.
10. Macaluso NJ, Glen RC. Exploring the 'RPRL' motif of apelin-13 through molecular simulation and biological evaluation of cyclic peptide analogues. *ChemMedChem*. 2010;5:1247–1253. doi: 10.1002/cmdc.201000061.
11. Deng C, Chen H, Yang N, Feng Y, Hsueh AJ. Apela regulates fluid homeostasis by binding to the APJ receptor to activate Gi signaling. *J Biol Chem*. 2015;290:18261–18268. doi: 10.1074/jbc.M115.648238.
12. Perjés Á, Kilpiö T, Ulvila J, Magga J, Alakoski T, Szabó Z, Vainio L, Halmetoja E, Vuolteenaho O, Petäjä-Repo U, Szokodi I, Kerkelä R. Characterization of apela, a novel endogenous ligand of apelin receptor, in the adult heart. *Basic Res Cardiol*. 2016;111:2. doi: 10.1007/s00395-015-0521-6.
13. Ho L, Tan SY, Wee S, Wu Y, Tan SJ, Ramakrishna NB, Chng SC, Nama S, Szczerbinska I, Sczerbinska I, Chan YS, Avery S, Tsuneyoshi N, Ng HH, Gunaratne J, Dunn NR, Reversade B. ELABELA is an endogenous growth factor that sustains hESC self-renewal via the PI3K/AKT pathway. *Cell Stem Cell*. 2015;17:435–447. doi: 10.1016/j.stem.2015.08.010.
14. Wang Z, Yu D, Wang M, Wang Q, Kouznetsova J, Yang R, Qian K, Wu W, Shuldiner A, Sztalryd C, Zou M, Zheng W, Gong DW. Elabela-apelin receptor signaling pathway is functional in mammalian systems. *Sci Rep*. 2015;5:8170. doi: 10.1038/srep08170.
15. Scimia MC, Hurtado C, Ray S, Metzler S, Wei K, Wang J, Woods CE, Purcell NH, Catalucci D, Akasaka T, Bueno OF, Vlasuk GP, Kaliman P, Bodmer R, Smith LH, Ashley E, Mercola M, Brown JH, Ruiz-Lozano P. APJ acts as a dual receptor in cardiac hypertrophy. *Nature*. 2012;488:394–398. doi: 10.1038/nature11263.
16. El Messari S, Iturrioz X, Fassot C, De Mota N, Roesch D, Llorens-Cortes C. Functional dissociation of apelin receptor signaling and endocytosis: implications for the effects of apelin on arterial blood pressure. *J Neurochem*. 2004;90:1290–1301. doi: 10.1111/j.1471-4159.2004.02591.x.
17. Kleinz MJ, Skepper JN, Davenport AP. Immunocytochemical localisation of the apelin receptor, APJ, to human cardiomyocytes, vascular smooth muscle and endothelial cells. *Regul Pept*. 2005;126:233–240. doi: 10.1016/j.regpep.2004.10.019.
18. Mayadas T, Wagner DD, Simpson PJ. von Willebrand factor biosynthesis and partitioning between constitutive and regulated pathways of secretion after thrombin stimulation. *Blood*. 1989;73:706–711.
19. Chandra SM, Razavi H, Kim J, Agrawal R, Kundu RK, de Jesus Perez V, Zamanian RT, Quertermous T, Chun HJ. Disruption of the apelin-APJ system worsens hypoxia-induced pulmonary hypertension. *Arterioscler Thromb Vasc Biol*. 2011;31:814–820. doi: 10.1161/ATVBAHA.110.219980.
20. Szokodi I, Tavi P, Földes G, Voutilainen-Myllylä S, Ilves M, Tokola H, Pikkarainen S, Piuhola J, Rysä J, Tóth M, Ruskoaho H. Apelin, the novel endogenous ligand of the orphan receptor APJ, regulates cardiac contractility. *Circ Res*. 2002;91:434–440.
21. Perjés Á, Skoumal R, Tenhunen O, Kónyi A, Simon M, Horváth IG, Kerkelä R, Ruskoaho H, Szokodi I. Apelin increases cardiac contractility via protein kinase Cε- and extracellular signal-regulated kinase-dependent mechanisms. *PLoS One*. 2014;9:e93473. doi: 10.1371/journal.pone.0093473.
22. Berry MF, Pirolli TJ, Jayasankar V, Burdick J, Morine KJ, Gardner TJ, Woo YJ. Apelin has *in vivo* inotropic effects on normal and failing hearts. *Circulation*. 2004;110(11 suppl 1):II187–II193. doi: 10.1161/01.CIR.0000138382.57325.5c.
23. Ashley EA, Powers J, Chen M, Kundu R, Finsterbach T, Caffarelli A, Deng A, Eichhorn J, Mahajan R, Agrawal R, Greve J, Robbins R, Patterson AJ, Bernstein D, Quertermous T. The endogenous peptide apelin potently improves cardiac contractility and reduces cardiac loading in vivo. *Cardiovasc Res*. 2005;65:73–82. doi: 10.1016/j.cardiores.2004.08.018.
24. Japp AG, Cruden NL, Barnes G, van Gemeren N, Mathews J, Adamson J, Johnston NR, Denvir MA, Megson IL, Flapan AD, Newby DE. Acute cardiovascular effects of apelin in humans: potential role in patients with chronic heart failure. *Circulation*. 2010;121:1818–1827. doi: 10.1161/CIRCULATIONAHA.109.911339.
25. Goetze JP, Rehfeld JF, Carlsen J, Videbaek R, Andersen CB, Boesgaard S, Friis-Hansen L. Apelin: a new plasma marker of cardiopulmonary disease. *Regul Pept*. 2006;133:134–138. doi: 10.1016/j.regpep.2005.09.032.
26. Kim J, Kang Y, Kojima Y, Lighthouse JK, Hu X, Aldred MA, McLean DL, Park H, Comhair SA, Greif DM, Erzurum SC, Chun HJ. An endothelial apelin-FGF link mediated by miR-424 and miR-503 is disrupted in pulmonary arterial hypertension. *Nat Med*. 2013;19:74–82. doi: 10.1038/nm.3040.
27. Alastalo TP, Li M, Perez Vde J, Pham D, Sawada H, Wang JK, Koskenvuo M, Wang L, Freeman BA, Chang HY, Rabinovitch M. Disruption of PPARγ/β-catenin-mediated regulation of apelin impairs BMP-induced mouse and human pulmonary arterial EC survival. *J Clin Invest*. 2011;121:3735–3746. doi: 10.1172/JCI43382.
28. Falcão-Pires I, Gonçalves N, Henriques-Coelho T, Moreira-Gonçalves D, Roncon-Albuquerque R Jr, Leite-Moreira AF. Apelin decreases myocardial injury and improves right ventricular function in monocrotaline-induced pulmonary hypertension. *Am J Physiol Heart Circ Physiol*. 2009;296:H2007–H2014. doi: 10.1152/ajpheart.00089.2009.

Elabela/Toddler Is an Endogenous Agonist of the Apelin APJ Receptor in the Adult Cardiovascular System, and Exogenous Administration of the Peptide Compensates for the Downregulation of Its Expression in Pulmonary Arterial Hypertension

Peiran Yang, Cai Read, Rhoda E. Kuc, Guido Buonincontri, Mark Southwood, Rubben Torella, Paul D. Upton, Alexi Crosby, Stephen J. Sawiak, T. Adrian Carpenter, Robert C. Glen, Nicholas W. Morrell, Janet J. Maguire and Anthony P. Davenport

Circulation. 2017;135:1160-1173; originally published online January 30, 2017;
doi: 10.1161/CIRCULATIONAHA.116.023218
Circulation is published by the American Heart Association, 7272 Greenville Avenue, Dallas, TX 75231

Print ISSN: 0009-7322. Online ISSN: 1524-4539

SUPPLEMENTAL MATERIAL

Elabela/Toddler is an endogenous agonist of the apelin APJ receptor in the adult cardiovascular system, and exogenous administration of the peptide compensates for the downregulation of its expression in pulmonary arterial hypertension

First author's surname: Yang

Short title: Down-regulation of Elabela/Toddler in PAH

Peiran Yang[1] MA, Cai Read[1] MRes, Rhoda E Kuc[1] BA, Guido Buonincontri[2] PhD, Mark Southwood[3] PhD, Rubben Torella[4] PhD, Paul D Upton[5] PhD, Alexi Crosby[5] PhD, Stephen J Sawiak[2] PhD, T Adrian Carpenter[2] PhD, Robert C Glen[4,6] PhD, Nicholas W Morrell[5] MD, Janet J Maguire*[1] PhD, Anthony P Davenport*[1] PhD

[1]Experimental Medicine and Immunotherapeutics, University of Cambridge, Level 6, Centre for Clinical Investigation, Box 110, Addenbrooke's Hospital, Cambridge, CB2 0QQ, U.K. [2]Wolfson Brain Imaging Centre, Department of Clinical Neuroscience, University of Cambridge, Box 65, CB2 0QQ, Cambridge, U.K. [3]Department of Pathology, Papworth Hospital, Papworth Everard, Cambridge, CB23 8RE, U.K. [4]Unilever Centre for Molecular Sciences Informatics, Department of Chemistry, University of Cambridge, Lensfield Road, Cambridge, CB2 1EW, U.K. [5]Department of Medicine, University of Cambridge, Box 157, Addenbrooke's Hospital, Cambridge, CB2 0QQ, U.K. [6]Biomolecular Medicine, Department of Surgery and Cancer, Imperial College, London, SW7 2AZ, U.K.

†The new address of G.B. is Istituto Nazionale di Fisica Nucleare, Sezione di Pisa, Edificio C, Largo Bruno Pontecorvo, 3, 56127, Pisa, Italy.

Corresponding author: Dr. Anthony Davenport

Experimental Medicine and Immunotherapeutics,

University of Cambridge,

Level 6, Centre for Clinical Investigation,

Box 110, Addenbrooke's Hospital,

Cambridge, CB2 0QQ, UK.

Phone: +44 (0)1223 336899

Fax: +44 (0)1223 761576

Email: apd10@medschl.cam.ac.uk

* Joint last authors

Supplemental Methods

Human tissues samples were obtained with informed consent (Papworth Hospital Research Tissue Bank REC08/H0304/56) and local ethical approval (REC05/Q0104/142). All rodent experiments were performed according to the local ethics committee (University of Cambridge Animal Welfare and Ethical Review Body) and Home Office (UK) guidelines under the 1986 Scientific Procedures Act.

Comptutational Methods

Molecular dynamics simulation of ELA-11 binding to the apelin receptor was conducted as previously described[1]. Briefly, the modelling template was based on a modified 2.5 Å resolution crystal structure of the human CXCR4 chemokine receptor (PDB code 3ODU[2]). MODELLER 9v8[3] was used for generating homology models of apelin. ELA-11 has been computationally designed using the SCHRÖDINGER software suite[4]. The apelin receptor and ELA-11 were used as a starting point for further docking analysis, using GOLD v5.1[5, 6]. An in-house script was created to create a constraint between the side-chains of F257 and W261 in the apelin receptor (predicted to interact with the C-terminal Phe of apelin and critical for receptor internalization[7]) and F10 in ELA-11 that greatly reduced the search space for docking, resulting in a pose consistent with current mutagenesis data[8]. No other constraints were applied to the complex. Images and diagrams were made to show peptide docking in the binding site using Pymol (Schrödinger, LLC) and key close contacts ELA-11 and the apelin receptor[9].

Human Tissue Collection

Human tissue samples were collected with local ethical approval and informed consent and were frozen and stored at -70ºC until use. Left ventricle (LV) and RV was from six normal

donor hearts for which there were no suitable recipients and LV was additionally obtained from fourteen patients transplanted for cardiomyopathy. LV and right ventricle (RV) was from six patients with pulmonary arterial hypertension (PAH). Histologically normal lung tissue and pulmonary artery were from patients undergoing lobectomy, additional lung tissue was collected from four patients with PAH. Coronary artery and aorta were collected from dilated cardiomyopathy patients. Saphenous vein, left internal mammary artery and radial artery were from patients receiving coronary artery bypass graft surgery. Human plasma samples were collected from healthy volunteers.

Comptetition Binding Experiments

For structure activity studies competition binding experiments were conducted in triplicate in homogenate of pooled human LV from cardiomyopathy patients as previously described[1]. Homogenate of human LV was incubated for 90 min with 0.1nmol/L [Glp^{65},Nle^{75},Tyr^{77}] [^{125}I]apelin-13 in assay buffer (mmol/L: Tris 50, $MgCl_2$ 5, pH 7.4, 22ºC), in the presence of increasing concentrations of human ELA-32, ELA-21, ELA-11 or [Pyr^{1}]apelin-13 peptides (0.5pmol/L-10µmol/L) (n=3 each). Non-specific binding was defined using 1µmol/L [Pyr^{1}]apelin-13. Equilibrium was broken by centrifugation (20,000g for 10 min, 4ºC). Pellets were washed with Tris-HCl buffer (50 mmol/L, pH 7.4, 4 ºC), re-centrifuged and bound radioactivity in final pellets counted. Data from triplicate experiments were analyzed using the iterative non-linear curve fitting programs EBDA and LIGAND (KELL package, Biosoft, UK) or GraphPad Prism6 and to derive values of affinity (expressed as the $-\log_{10}$ of the dissociation constant (pK_i ±sem)) and receptor density (B_{MAX}±sem). The pK_i and B_{MAX} values for the three putative endogeous forms of ELA (ELA-32, ELA-21 and ELA-11) were compared using ANOVA with Tukey's post tests. The synthetic analogues ELA-14 and cyclo[1-6]ELA-11 were tested for affinity at the human apelin receptor expressed in CHO-K1 cells (data obtained from Cerep, Celle L'Evescault, France).

To investigate whether the affinity of ELA peptides or the density of ELA binding sites is altered in human PAH competition binding experiments were repeated as described above using ELA-21 as the competing ligand in LV and RV from pooled homogenate from six patients transplanted for PAH and LV and RV from six normal hearts as controls. Data from triplicate experiments were analyzed using the iterative non-linear curve fitting programs EBDA and LIGAND (KELL package, Biosoft, UK) to determine values of affinity (K_D) and receptor density (B_{MAX}). Values were compared for LV and RV between PAH and controls using Student's 2-tailed *t*-test.

Inhibition of cAMP Accumulation, β-Arrestin Recruitment and Receptor Internalisation Assays

Second messenger signalling and receptor pharmacology were studied in assays (DiscoveRx, Fremont, CA, USA) according to instructions from the manufacturer and as previously described[1]. 3-5 assays with 2-6 replicates each were performed.

For inhibition of forskolin-induced cAMP accumulation, CHO-K1 cells artificially expressing the human apelin receptor were seeded in Cell Plating medium into 96-well plates and incubated for 24 hours at 37ºC in 5% CO_2, followed by replacement of the medium with cAMP Antibody Reagent in Cell Assay Buffer. Basal levels of cAMP were elevated by 15μmol/L forskolin, which was incubated with the cells for 30 minutes at 37°C, in the absence or presence of human ELA-32, ELA-21, ELA-11, [Pyr^1]apelin-13, or two synthetic analogues, ELA-14 and cyclo[1-6]ELA-11, (1pmol/L-0.3μmol/L) diluted in Cell Assay Buffer. Cells were incubated with a mixture of Lysis Buffer, cAMP Buffer D and Detection Reagents for 1 hour incubation at room temperature, followed by a 3 hour incubation with cAMP Reagent A at room temperature, and chemiluminescence reading (LumiLITE^{TM} Microplate Reader,

DiscoveRx). Responses measured in relative light units were fitted to 4 parameter logistic concentration response curves in GraphPad Prism 6 (La Jolla, CA, USA) and values of potency, pD_2 ($-\log_{10} EC_{50}$ (where EC_{50} is the concentration producing half maximal response)), and maximum response (E_{MAX}) were calculated for each compound. Data were subsequently expressed normalised as percentage inhibition of forskolin-stimulated cAMP production.

β-Arrestin assays were conducted as previously described[1]. CHO-K1 cells artificially expressing the human apelin receptor were seeded in Cell Plating medium into 96-well plates and incubated for 48 hours at 37ºC in 5% CO_2. Human ELA-32, ELA-21, ELA-11, [Pyr[1]]apelin-13, or two synthetic analogues, ELA-14 and cyclo[1-6]ELA-11, (1pmol/L-3μmol/L) were diluted in Cell Plating medium and added to the cells for 90 minutes at 37ºC. . For antagonist experiments, additional 30-minute incubation was carried out prior to addition of agonists with 30μmol/L ML221[10] (Tocris Bioscience, Bristol, UK) made in Cell Plating medium. Detection reagents were then added for a 2-hour incubation at room temperature followed by chemiluminescence reading. Responses measured in relatve light units were fitted to 4 parameter logistic concentration response curves in GraphPad Prism 6 (La Jolla, CA, USA) and values of pD_2 ($-\log_{10} EC_{50}$) and maximum response (E_{MAX}) were calculated for each compound. Data were subsequently normalized to the maximum response to [Pyr[1]]apelin-13 used as the reference agonists in each assay. For antagonist experiments using a small molecule antagonist ML221[10], antagonist affinities, pA_2 ($-\log K_B$, where K_B is the antagonist dissociation constant) were determined for the apelin receptor.

Internalisation assays were conducted as previously described[1]. U2OS cells artificially expressing the human apelin receptor were seeded in Cell Plating medium in 96-well plates and incubated for 48 hours at 37ºC in 5% CO_2. Human ELA-32, ELA-21 or ELA-11, or [Pyr[1]]apelin-13 (0.1pmol/L-10μmol/L) were diluted in Cell Plating medium and incubated with

the cells for 3 hours at 37ºC. This was followed by incubation with the detection reagents for 90 minutes at room temperature and luminescence reading. Data were analysed as described for the β-arrestin assay.

Protein Phosphorylation and Angiogenesis Assays in Cultured PAEC and PASMC

Control pulmonary artery endothelial cells (PAECs, n=3) (Lonza) and control (n=3) and PAH (n=3) pulmonary artery smooth muscle cells (PASMCs) (from sex matched controls and patients with BMPRII mutations) were plated at 330,000/6cm dish and allowed to adhere. Cells were serum starved (0.1% fetal bovine serum) overnight, washed in PBS and subsequently treated for 10 minutes with either 0.1% serum (control) or [Pyr^{1}]apelin (100nmol/L) or ELA-32 (100nmol/L). Cells were then washed in PBS, lysed at 4°C for 30 minutes, centrifuged at 12,000g for 7.5 mins and lysates stored at -70°C prior to the assay. The relative levels of protein phosphorylation for an array of 43 kinase phosphorylation sites and 2 related total proteins were determined in duplicate using lysates (100ng protein per well) of the treated cells according to the manufacturer's instructions (Proteome Profiler Array, Human Phospho-Kinase Array Kit, Catalogue No. ARY003B, R&D Systems Inc. Minneapolis, USA). The assay was performed as directed by the manufacturer and membranes exposed for 3 minutes. Spot density was quantified using Image J and the average determined for the duplicate data. The appropriate negative control value was subtracted from all readings and data expressed as arbitary units (AU). Data were analysed by one-way ANOVA for repeated (matched) measures with Tukey's post test for multiple comparisons.

For angiogenesis assays, cells were plated at 60,000/well in 12 well plates. The conditioned media from the the same cells treated for 24 hours with 0.1% serum, [Pyr^{1}]apelin or ELA-32 (both 100nmol/L) was used to determine the relative levels of 55 secreted human angiogenesis-related proteins according to the manusfacturer's instructions (Proteome Profiler Array, Human

Angiogenesis Array Kit, Catalogue No. ARY007, R&D Systems Inc. Minneapolis, USA). Data were quantified and analysed as described for the phospho-kinase assay.

APELA mRNA Expression by Reverse Transcription and qPCR

The mRNA expression of *APELA* (gene for ELA) was studied in human cardiovascular tissues using reverse transcription and quantitative real-time PCR. For RNA extraction, cubes ($5mm^3$), or the equivalent amount, of human coronary (n=11), mammary (n=6), radial (n=9), and pulmonary artery (n=4), aorta (n=6), umbilical (n=6) and saphenous vein (n=6), LV (n=8), lung (n=6) were incubated with TRIzol® Reagent (Life Technologies, Paisley, UK) in metal bead lysing matrix (Lysing Matrix D for heart and lung tissues) (MP Biomedicals, Santa Ana, CA, USA), and homogenized using the FastPrep-24™ 5G system (MP Biomedicals) for up to 6 runs at 6.5m/s for 45 seconds. After homogenization, total RNA was extracted using PureLink™ RNA Mini Kit (Life Technologies) with DNase treatment included, performed according to the manufacturer's instructions. The yield of RNA was determined with NanoDrop 1000 spectrophotometer (Wilmington, DE, USA) and 1μg of RNA from each sample was used for reverse transcription with the Promega Reverse Transcription System (Promega, Madison, WI, USA), carried out according to manufacturer's instructions. The cDNA product was used in triplicates for real-time quantitative PCR was performed for 45 cycles using the ABI 7500 Real-Time PCR System (Life Technologies) with double-dye Taqman primer probes for human *APELA* gene from Primerdesign (Chandlers Ford, UK) and for human 18S rRNA (Life Technologies) as the internal control. The primer sequences or IDs are shown in Supplemental Table 1. The expression of *APELA* was normalised to that of 18S using the comparative C_q method[11].

Alteration in *APELA* mRNA expression in pulmonary arterial hypertension (PAH) was studied in lungs from three PAH and one pulmonary veno-occlusive disease (class 1' PAH) patients

and tissue from four histologically normal lungs. For comparison expression was also determined in tissue from two rodent models of PAH. Rat tissue from monocrotaline (MCT) treated animals was generously provided by Dr Benjamin Garfield (Imperial College London). Male Sprague-Dawley rats (208±3g) was given a subcutaneous injection of MCT (40mg/kg body weight) to induce PAH, or PBS (phosphate buffered saline) as controls (n=5 each). The animals were sacrificed by terminal anaesthesia and exsanguination three weeks after MCT injection and the heart was removed. Tissue from Sugen/hypoxia exposed (n=7) and weight matched control (n=6) animals was a kind gift from Emily Groves (Morrell Group, University of Cammbridge). Male Sprague-Dawley rats (150-200g) were given a subcutaneous injection of Sugen 5416 (20 mg/kg, Tocris, Bristol, UK), housed in hypoxic chambers at 10% O_2 for 3 weeks, followed by 8 weeks normoxia prior to euthanasia by exsanguination and removal of the heart. mRNA expression in the RV of these rats were compared with weight-matched controls. The RV was used to study *Apela*, *Aplnr* and *Apln* (genes for ELA, apelin receptor and apelin) mRNA expression, determined as desribed above using rat 18S rRNA as internal controls. The primer sequences or IDs are shown in Supplemental Table 1. Gene expression in MCT and PBS-injected animals were compared using unpaired Student's t test.

Endogenous ELA Peptide Expression Localized by Immunostaining

Dual-labelling immunofluorescent staining was conducted as described[7] using ELA antiserum that cross reacted with ELA peptides, but not apelin (Supplemental Figure 1), the endothelial marker von-Willebrand factor (vWF) (1:50) and frozen sections of human histologically normal blood vessels (n=3-6), LV (n=8), lung (n=7), and primary PAECs (n=3). Peroxidase (DAB) stained, formaldehyde fixed human lung sections from idiopathic or familial PAH patients (n=10) and controls (n=10) were scored as positive or negative for ELA staining in

100 blood vessels with diameter ≤100μm. The average proportions of ELA-positive and negative vessels were compared between normal and PAH sections using Fisher's exact test.

Immunostaining was carried out as previously described[12]. ELA peptide expression was studied using rabbit polyclonal primary antiserum against human [pGlu^{1}]ELA-32 (Phoenix Pharmaceuticals, Belmont, CA, USA). An ELISA was performed to confirm cross-reactivity of the primary antiserum with ELA peptides but not apelin. Briefly, a 96-well plate with non-specific binding blocked by incubation with 3% bovine serum albumin was coated with 1μg/mL human ELA-32, ELA-21, ELA-11, or [Pyr^{1}]apelin-13 (or uncoated control) overnight at 4°C. Following washes with phosphate buffered saline 0.1% Tween-20 (PBS/T), polyclonal swine anti-rabbit IgG conjugated with horseradish peroxidase (Dako, Glostrup, Denmark) was applied for 2 hours at room temperature. After further washing, 3,3',5,5'-tetramethylbenzidine substrate was added for 5 minutes for generation of a colored product. The reaction was then quenched with 1mol/L sulfuric acid and the plate was read for absorbance at 450nm (ELx800 Absorbance Microplate Reader, BioTek, Winooski, VT, USA). Concentration response curves were fitted in GraphPad Prism 6.

For dual-label immunofluorescence with human tissues; 10μm fresh-frozen sections of human coronary, mammary, radial, and pulmonary artery (n=3 each) and 30μm fresh-frozen sections of human LV (n=8) and lung (n=7). Sections were fixed in acetone for 10 minutes. Non-specific binding was blocked by incubation with 5% goat serum in PBS for 2 hours at room temperature. Rabbit polyclonal primary antiserum against human [pGlu^{1}]ELA-32 (1:50 for vessels, 1:100 for LV, 1:500 for lung) was applied together with a monoclonal mouse anti-human von-Willebrand factor antibody (1:50) (Dako), used as a marker for endothelial cells, in PBS/T containing 3% goat serum on the sections for overnight incubation at 4°C. The primary antisera was omitted on adjacent negative control sections. Following 3 washes in cold PBS/T,

Alexa Fluor® 488 donkey anti-rabbit IgG (1:100) and Alexa Fluor® 568 donkey anti-mouse IgG (1:100) (both from Life Technologies) were applied in PBS/T containing 3% donkey serum and incubated for 2 hours at room temperature. This was followed by washing and mounting with ProLong Gold® antifade reagent (Life Technologies), and imaging using a Leica TCS SP8 confocal laser scanning microscope (Leica Microsystems, Milton Keynes, UK). To study the expression of ELA peptide in endothelial cells, PAECs (Lonza, Basel, Switzerland) were cultured in EGM™-2 medium with 2% serum, and plated on coverslips at passage 7 for immunostaining (n=3). The cells were fixed in methanol/acetone and the staining was conducted as above. All images were processed in the same method using Fiji[13, 14] for background subtraction using the rolling ball method, histogram stretching and merging of the channels.

ELA expression in blood vessels in normal and PAH human lung sections was investigated as previously described[15]. Peroxidase/DAB staining was carried out using human lung sections from idiopathic or familial PAH patients (n=10) and controls (n=10). Tissues were fixed with formaldehyde, cut into 10µm sections and processed for antigen retrieval using the Dako PT Link instrument according to manufacturer's instructions. Non-specific binding was blocked by incubation with 5% goat serum in PBS for 2 hours at room temperature. Rabbit polyclonal primary antiserum against human [pGlu[1]]ELA-32 (1:500) in PBS/T containing 3% goat serum on the sections for overnight incubation at 4°C. Following 3 washes in cold PBS/T, sections were incubated for 1 hour with 1:100 goat anti-rabbit IgG antibody, washed again, and incubated for 1 hour with 1:200 rabbit PAP complex. After repeated washing in PBS/T, 3,3-diaminobenzidine in 0.1M Tris-HCl with 3% hydrogen peroxide was applied for 4 minutes. Then the tissues were dehydrated through an alcohol series and cleared in xylene, and mounted with DePeX medium (VWR International Ltd, Lutterworth, UK). Blood vessels with a diameter ≤100µm were scored blindedly as positive or negative for ELA staining at 375x

magnification on a Polyvar Met microscope (Reichert Technologies, Munich, Germany), with 100 vessels counted from each section. The average number of ELA-positive and negative vessels were compared between normal and PAH sections using Fisher's exact test in GraphPad Prism 6.

Enzyme Immunoassays

For detection of ELA peptide levels in plasma human blood was collected from healthy volunteers (n=25, 20 male and 5 female, age=30±2 years) into heparinised tubes and centrifuged at 2000xg for 5 minutes to extract plasma. Concentrations of apelin peptides were measured using a widely used enzyme immunoassay (EK-057-23, Phoenix Pharmaceuticals)[1, 16] and concentrations of ELA peptides were measured using a selective immunoassay from the same manufacturer (EK-007-19, Phoenix Pharmaceuticals), following manufacturer's instructions. Briefly, all samples were assayed in duplicates and diluted 1:2 in the assay buffer to minimise interference. Samples were added to wells of a secondary antibody-coated plate and incubated with primary antibody and competing biotinylated peptide for 2 hours at room temperature with orbital shaking. The wells were then washed and streptavidin-horseradish peroxidase added to incubate for an hour. Following another washing, the enzyme substrate solution was added and incubated for an hour. The reaction was quenched by adding hydrochloric acid and the plate was read on the plate reader for absorbance at 450nm. The absorbance was proportional to the amount of biotinylated peptide-peroxidase complex and therefore inversely proportional to the amount of peptied in the samples. The unknown concentration in samples were determined by extrapolation to a standard curve of known concentrations and multiplying by the dilution factor. The calculated concentrations of ELA and apelin were compared using Student's t test and tested for correlation using Pearson's test in GraphPad Prism 6.

For detection of changes in plasma cardiovascular peptides in response to ELA-32 administration, plasma from either ELA-32 or saline control treated rats was collected in EDTA tubes and centrifuged at 2000xg for 5 minutes to extract plasma. Angiotensin –II (Catalogue no. EKE-002-12) and BNP-32 (Catalogue no. EK-011-14) levels were measured using specific enzyme immunoassays according to the maufacturer's instructions (Phoenix Pharmaceuticals , Inc. CA, USA) as described above.

Effects of ELA and Apelin *in vivo*

The cardiac effects of ELA and apelin *in vivo* was first studied using magnetic resonance imaging (MRI), as previously described[17]. Male Sprague Dawley rats (264±2g) were anaesthetised with gaseous isoflurane both for induction (3% in 1.5 L/min oxygen) and maintenance (1.5-2.5% in 1.5 L/min oxygen). For compound administration, the right external jugular vein was cannulated with polyethylene tubing (Smiths Medical, Ashford, UK) filled with heparinised 0.9% saline solution. A pressure sensor for respiration rate was used to monitor depth of anaesthesia, with respiration rate was maintained at 45-55 breaths per minute. Body temperature was monitored using a rectal thermometer and maintained at 37°C using a flowing-water heating blanket. Prospective gating of the MRI sequences was achieved with electrocardiography monitoring using paediatric ECG electrodes (3M Europe, Diegem, Belgium) on left and right forepaws. MRI was performed at 4.7 T with a Bruker BioSpec 47/40 system (Bruker Inc., Ettlingen, Germany). A birdcage coil of 12cm was used for signal excitation and animals were positioned prone over a 2cm surface coil for signal reception. After initial localisation images, 4-chamber and 2-chamber views were obtained. Using these scans as a reference, short axis slices were acquired (FISP, TR/TE 6 ms/2.1 ms, 20-30 frames, 5 cm FOV, 256x256 matrix, 2 mm slice thickness, bandwidth 78 kHz, flip angle 20°, NEX 2), perpendicularly to both the long-axis views. Full LV and RV coverage in the short axis was achieved with no slice gap with 9-10 slices. After acquiring this reference baseline scan, ELA-

32 (20 and 150nmol, n=8), [Pyr^{1}]apelin-13 (50 and 650nmol, n=5) or the same volume (500µl) of saline (n=6) was administered as two cumulative bolus intravenous injections through the implanted cannula and flushed with 100µL saline. Following the injections, three mid-ventricular slices were planned in the short axis of the heart in order to capture changes in function with a 1.5 min resolution. (FISP, TR/TE 6 ms/2.1 ms, 20-30 frames, 5 cm FOV, 128x128 matrix, 2 mm slice thickness, bandwidth 78 kHz, flip angle 20°, NEX 1). The effects of the compounds were monitored for no less than 10 minutes. Delineation of the LV and RV was as described using Segment v1.9[17, 18]. Measurements made from the three slices were normalised to the baseline scan to estimate the volumes at end-systolic and end-diastolic points. The LV and RV ejection fraction was calculated and expressed as change from baseline. The peak effects induced by ELA, apelin and saline were tested using one-way ANOVA with Dunnett's post-test comparing ELA and apelin groups to the saline group using GraphPad Prism 6.

The MRI study of the *in vivo* cardiac effects of ELA and apelin was complemented by catheterization experiments. The surgical part of the experiment was performed as previously described[19]. Male Sprague Dawley rats (257±7g) anaesthetised with gaseous isoflurane (3% for induction and 1.5-2% for maintenance, 1.5L/min oxygen). Body temperature was monitored using a rectal thermometer and maintained at 37°C. For compound administration, the right external jugular vein was cannulated with polyethylene tubing (Smiths Medical) filled with heparinised 0.9% saline solution. A pressure volume catheter (SPR-869, Millar, ADIstruments, Oxford, UK) was connected to the data PowerLab 16/35 system with LabChart 8 (ADIstruments, Oxford, UK) and calibrated using the MPVS Ultra PV Unit (ADIstruments, Oxford, UK). Then the catheter was inserted into the LV via the right carotid artery. The position of the catheter was determined by the blood pressure and shape of the pressure volume loops. The animal was allowed to stabilise for recording of baseline hemodynamic parameters.

ELA-32 (20 and 150nmol, n=10), [Pyr^{1}]apelin-13 (50, 400 and 1300nmol, n=8) or the equal volume (500µl) of saline (n=6) were given as cumulative bolus intravenous injections via the cannula, which was flushed with 100µL saline. The effects of the compounds were monitored for no less than 10 minutes. Data analysis was performed using LabChart 8 as previously described[20]. The peak effects of ELA, apelin and saline on LV systolic pressure, cardiac output, contractility (dP/dt_{MAX}) were expressed as change from baseline and tested using one-way ANOVA with Dunnett's post-test comparing ELA and apelin groups to the saline group using GraphPad Prism 6.

Monocrotaline-Induced Rat Model of PAH

Methods were as previously described[21]. Male Sprague-Dawley rats (205±2g) were randomly allocated to receive MCT (n=18; 60mg/kg body weight) or an equal volume of vehicle (n=17; 0.9% saline) by subcutaneous injection on day 0. From day 1 to day 21, randomly selected MCT (n=9) and vehicle control (n=9) exposed animals received daily intraperitoneal injections of ELA-32 (450µg/kg body weight) with the remainder (MCT, n=9; saline, n=8) receiving intrperitoneal injections of saline for 21 days. On day 21, the rats were weighed and catheterized for right ventricular hemodynamic measurements as previously described[21, 22]. Briefly, rats were anaesthetized with gaseous isoflurane (3% for induction, 1.5-2.5% for maintenance, 1.5 L/min oxygen). A pressure volume catheter (SPR-869, Millar) connected to the data PowerLab 16/35 system with LabChart 5 and calibrated using the MPVS Ultra PV Unit was inserted into the right ventricle via the right external jugular vein to measure right ventricular systolic pressure (RVSP). To investigate any effect of chronic ELA administration on systemic blood pressure, carotid artery and LV catheterization was performed in ELA control and saline control animals (n=5 each group) as described above. The position of the catheter was determined by the blood pressure and shape of the pressure volume loops. Then the rats were euthanized by exsanguination, terminal blood samples were collected into EDTA

tubes for determination of plasma levels of angiotensin-II and BNP-32. The left lung infused with 0.8% agarose to inflate, removed, fixed in 10% formalin (CellPath, Powys, UK), paraffin embedded and stained for smooth muscle α-actin and elastic van Giesen as described[21, 22]. Other tissues collected included the heart, the RV was dissected from the LV+septum and the weight ratio of these (RV compared to LV+septum), also known as the Fulton index, was determined as a measure of right ventricular hypertrophy. Paraffin embedded sections of RV were compared for evidence of cardiomyocyte hypertrophy or proliferation by measuring cardiomyocyte cross-sectional area of at least 100 cardiomyocytes in at least six myocardial zones per section stained with FITC conjugated WGA (wheat germ agglutinin) using 'threshhold and analyze particle' tool in ImageJ. Additionally, the average number of cardiomyocyte nuclei/area and number of GATA4 positive nuclei/area[23] were counted in five different myocardial zones. In order to compare size and numbers of cells accurately between zones and between tissue sections, only cells in one particular orientation were included. In the left lung small (diameter 25-75μm) pulmonary blood vessels associated with alveolar ducts were scored as completely muscular, partially muscular, or non-muscular with 100 vessels scored from each section. Statistical significance was assessed by comparing the percentage of fully muscularized vessels between groups. The wall thickness of pulmonary arteries (diameter >75μm) close to terminal bronchioles was determined by measuring the average wall thickness as a percentage of average lumen diameter of the vessel using ImageJ as previously described[21]. Group data were compared using one-way ANOVA with Tukey's post-test.

Materials

Human [Pyr^1]apelin-13 were synthesized by Severn Biotech (Kidderminster, UK). Human ELA-32 (the [$pGlu^1$]ELA-32 form) was synthesized by Severn Biotech or purchased from Phoenix Pharmaceuticals. Human ELA-21 and ELA-11 were from Phoenix Pharmaceuticals (Belmont, CA, USA). ELA-14 and cyclo[1-6]ELA-11 were synthesized by Department of

Chemistry, University of Cambridge. All other reagents were from Sigma-Aldrich Ltd (Poole, UK), unless otherwise stated.

Supplemental Table

Supplemental Table 1: Primer sequences or IDs for RT-qPCR.

Target	Primer Sequences
Human *APELA*	Sense GAAGAAGAAGAGGAGTGAAGGA Antisense CCATTCCAGGTGCTTTCAAAT
Rat *Apela*	Sense AGTCACTGATCTCCTTGGTTACC Antisense CTGCCGCACTGTTGCCA
Primers from Thermofisher	
Target	Primer Assay ID
Human 18S rRNA	Hs99999901_s1
Rat 18S rRNA	Rn03928990_g1
Rat *Aplnr*	Rn00580252_s1
Rat *Apln*	Rn00581093_m1

Supplemental Results and Figures

Cross-Reactivity Testing of the Human ELA Antiserum

As expected, the antiserum showed similar cross-reactivity to human ELA-32, ELA-21 and ELA-11 peptides but did not cross-react with human [Pyr[1]]apelin-13 peptide (Supplemental Figure 1). Therefore it can be used as an ELA-specific antiserum.

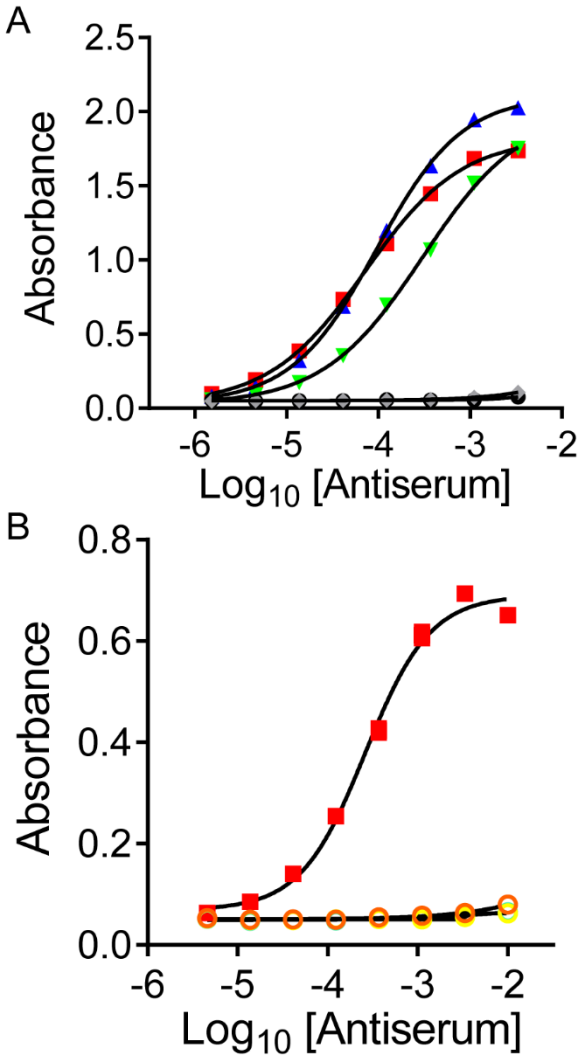

Supplemental Figure 1. Custom ELISA confirms cross-reactivty and specificity of the ELA antibody. Cross reactivity to (A) ELA-32 (■), ELA-21 (▲), ELA-11 (▼), but not to [Pyr[1]]apelin-13 (●) or uncoated controls (◆). (B) Compared to ELA (■), no cross reactivity was obtained with other cardiovascular peptides; angiotensin II (○), bradykinin (○), endothelin-1 (○).

Effect of [Pyr[1]]Apelin-13 and ELA-32 on Levels of Protein Phosphorylation in PAEC and PASMCs *in vitro*

There were significant increases in phosphorylation levels of ERK1/2 and eNOS in response to [Pyr[1]]apelin-13 (100nmol/L) or ELA-32 (100nmol/L) in cultured PAECs.

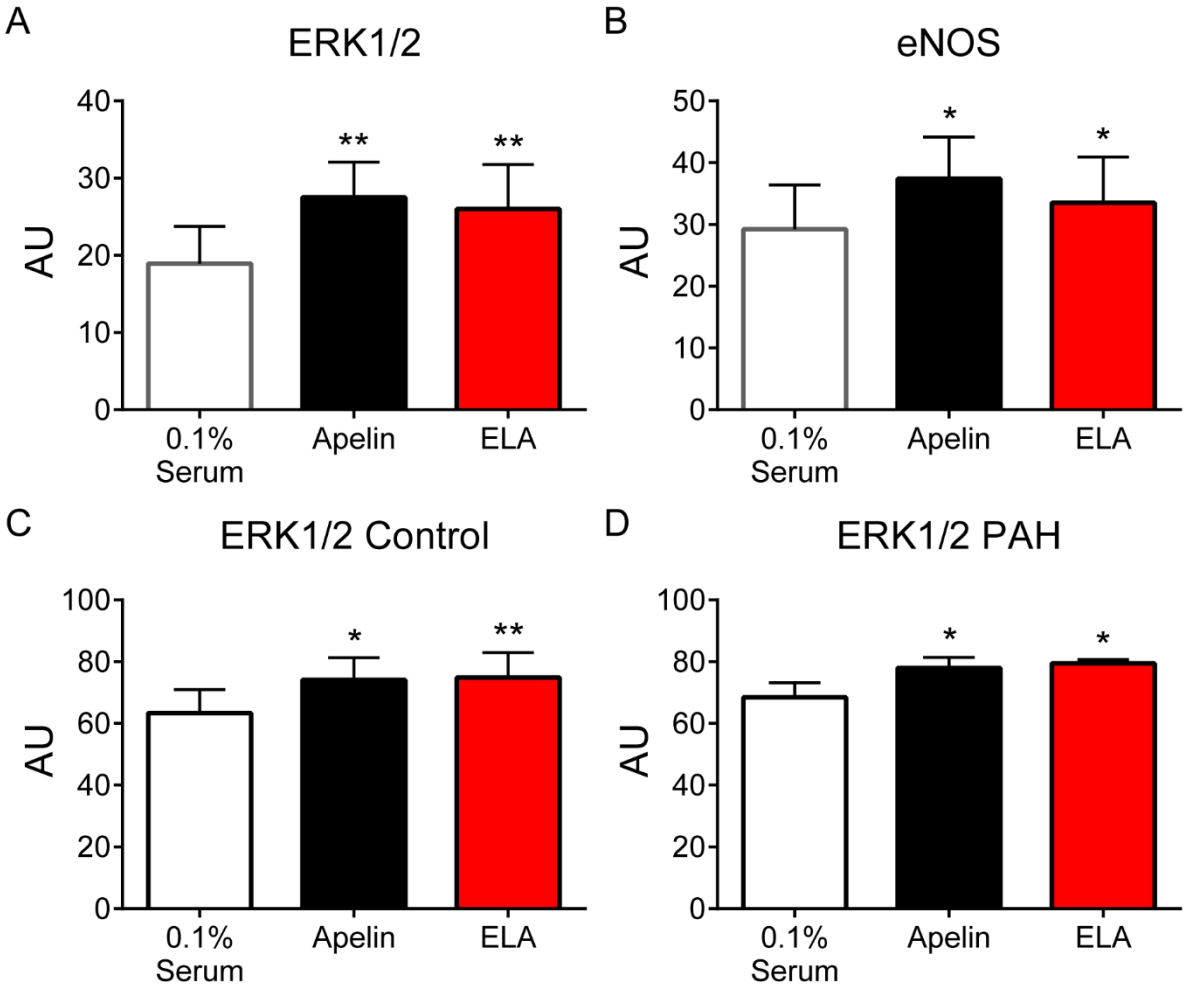

Supplemental Figure 2. Effect of [Pyr[1]]Apelin-13 and ELA-32 on levels of protein phosphorylation in PAEC and PASMCs *in vitro*. Increased phosphorylation levels of (A) ERK1/2 and (B) eNOS in PAECs and ERK1/2 in (C) control and (D) PAH PASMcs following treatment with 0.1% serum (control), [Pyr[1]]apelin-13 or ELA-32 (both 100nmol/L). Significantly different from control * P≤0.05, **P≤0.01, one-way ANOVA for repeated measures with Tukey's post-test for multiple comparisons.

There was no significant effect on level of phosphorylation of either peptide on an additional 41 kinases and 2 total proteins (Supplemental Figure 3).

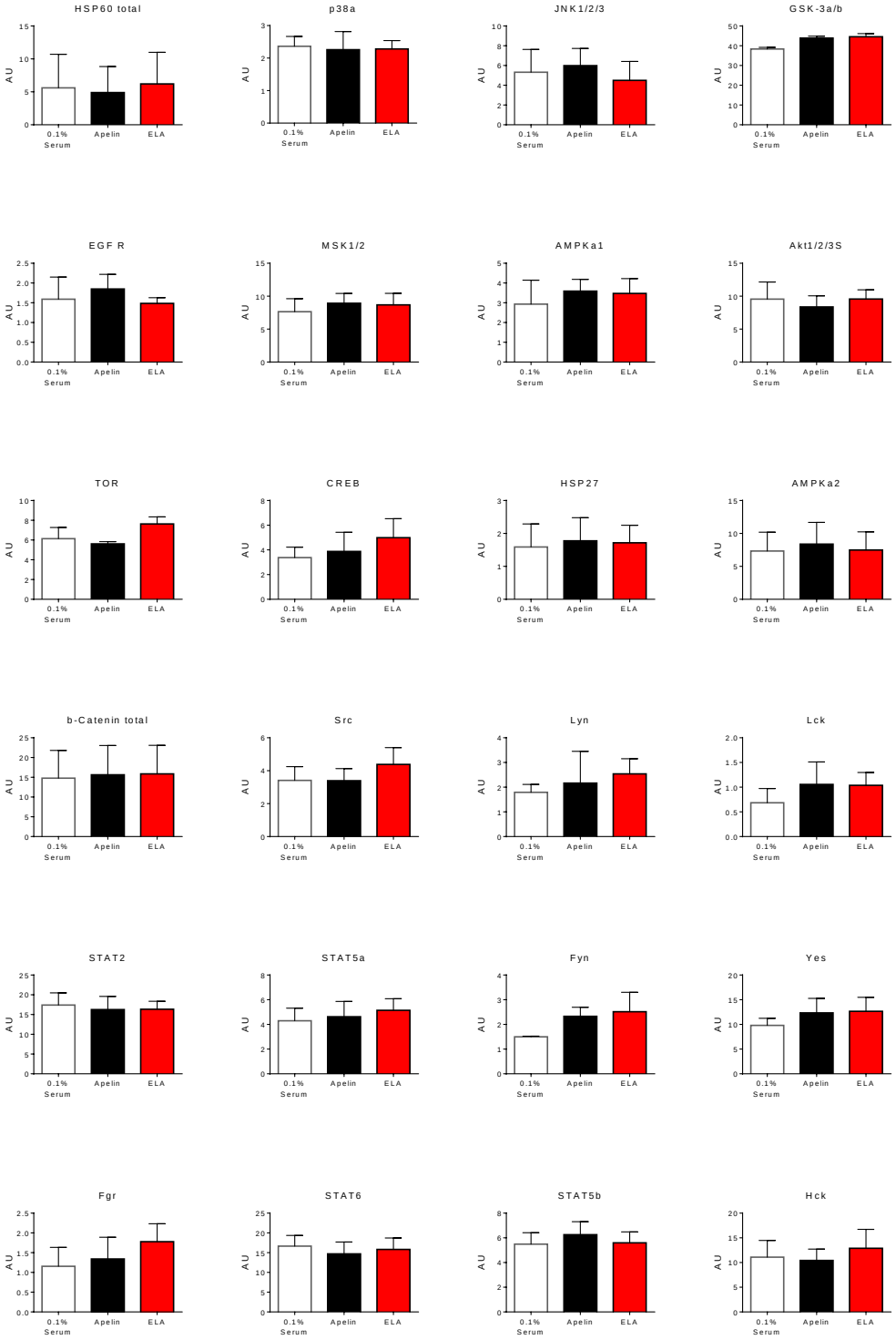

Supplemental Figure 3. Lack of effect of [Pyr[1]]apelin-13 and ELA-32 on protein phosphorylation levels.

Supplemental Figure 3 continued.

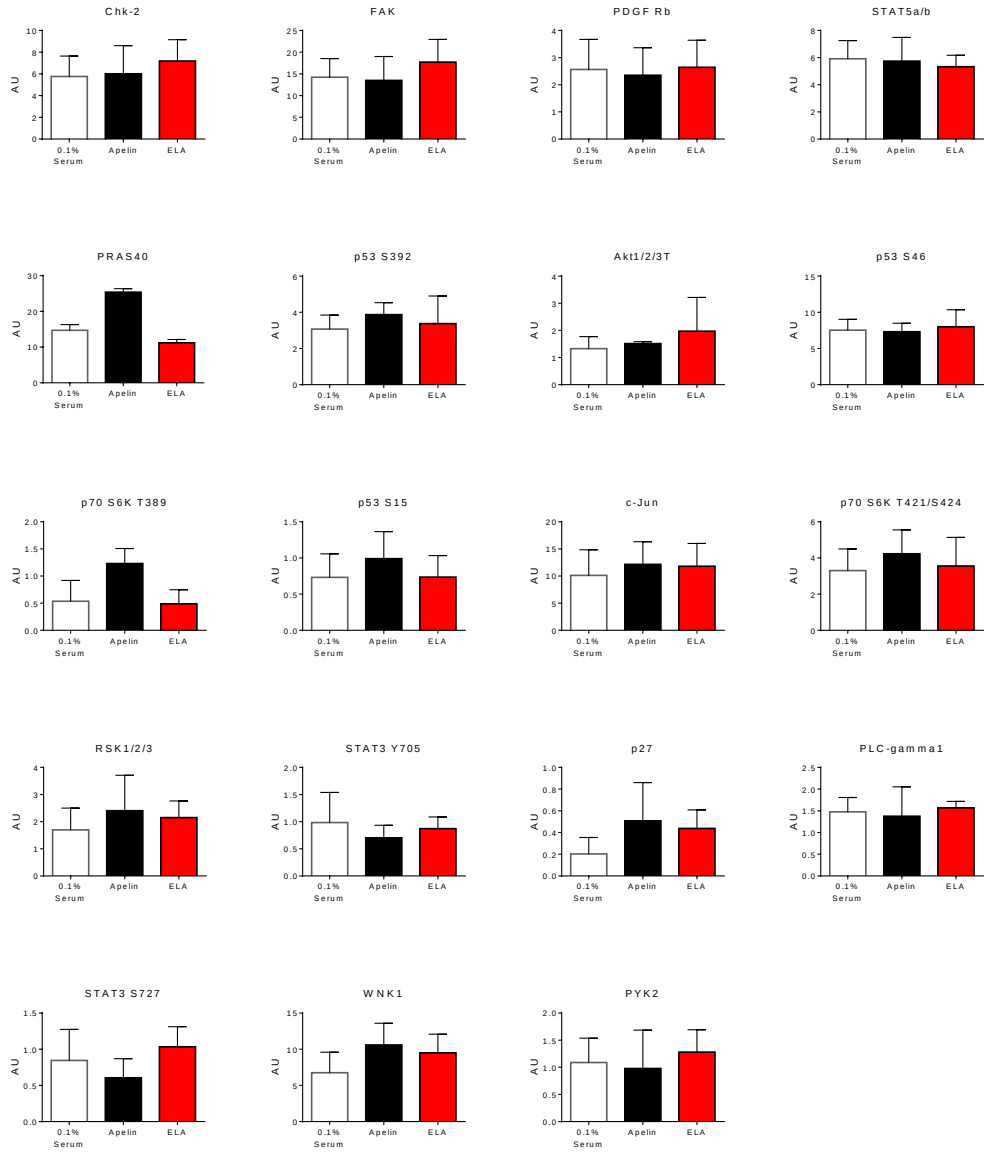

There were no significant changes in levels of secreted angiogenesis factors in response to [Pyr^{1}]apelin (100nmol/L) or ELA-32 (100nmol/L) treatment in either PAECs (Supplemental Figure 4) or control/PAH PASMCs (Supplemental Figure 5).

Supplemental Figure 4. Lack of effect of [Pyr^{1}]Apelin-13 and ELA-32 on levels of secreted angiogenesis factors in cultured PAECs.

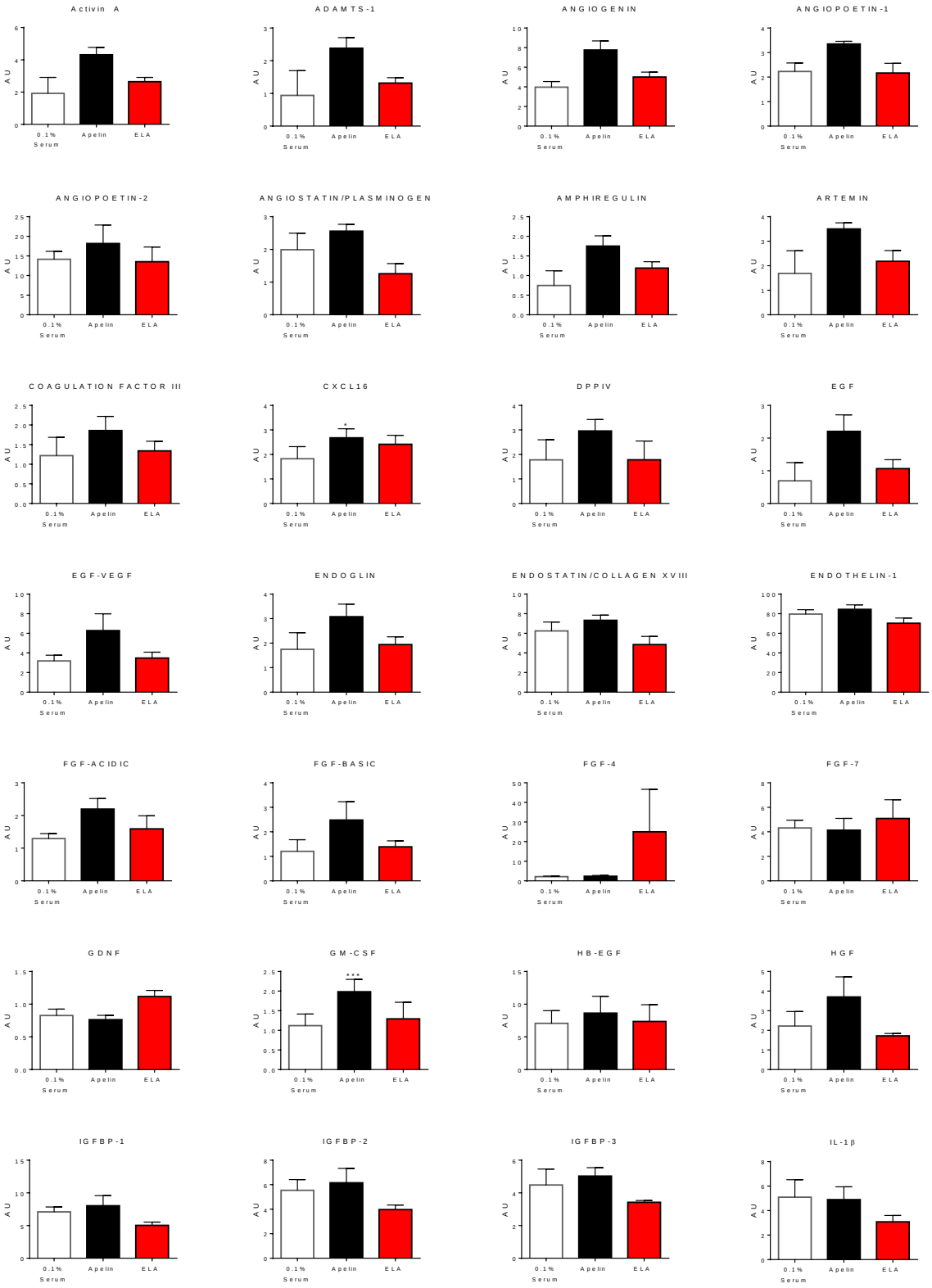

Supplemental Figure 4 continued

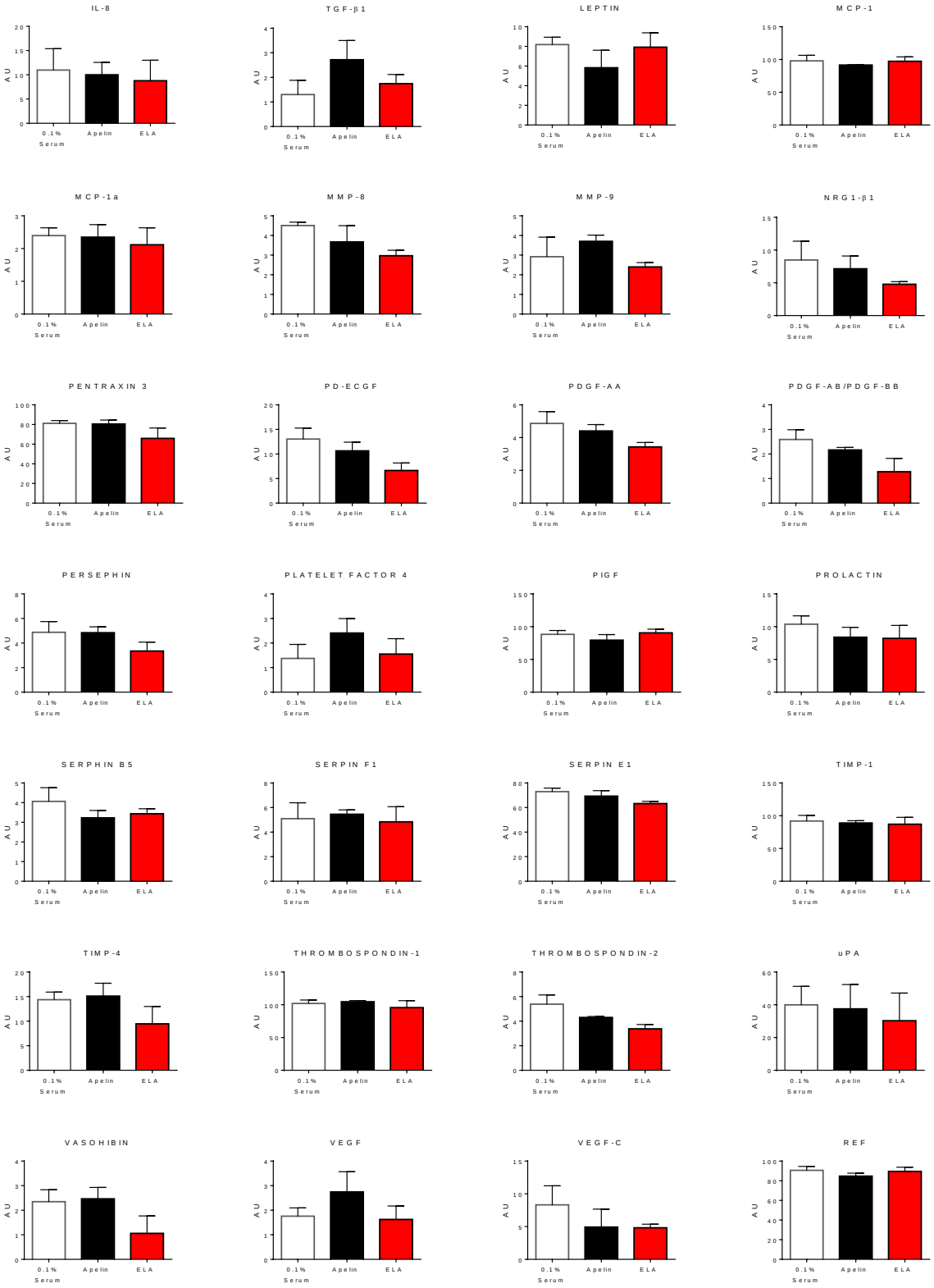

Supplemental Figure 5. Lack of effect of [Pyr[1]]Apelin-13 and ELA-32 on levels of secreted angiogenesis factors in cultured control and PAH PASMCs.

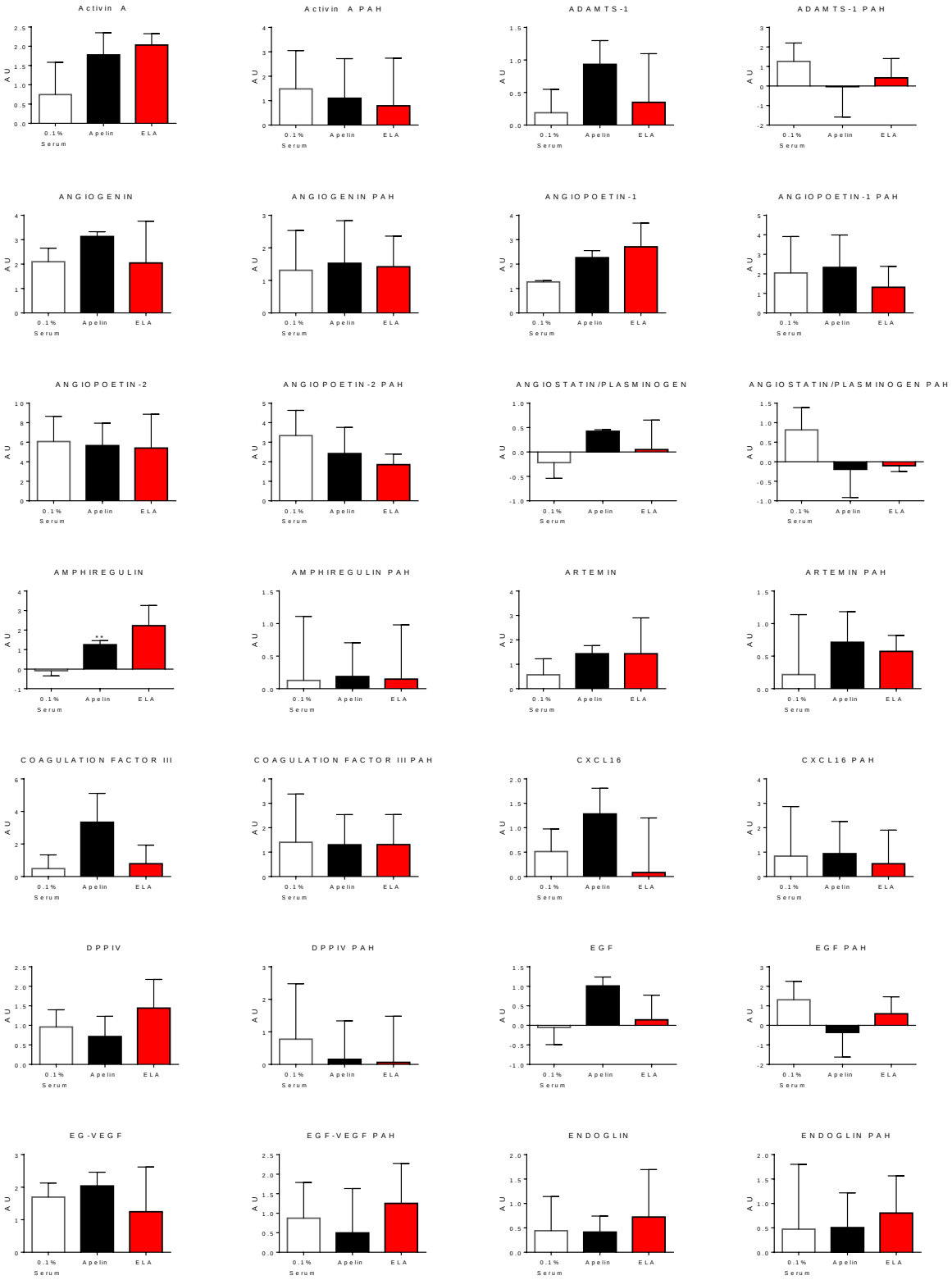

Supplemental Figure 5 continued.

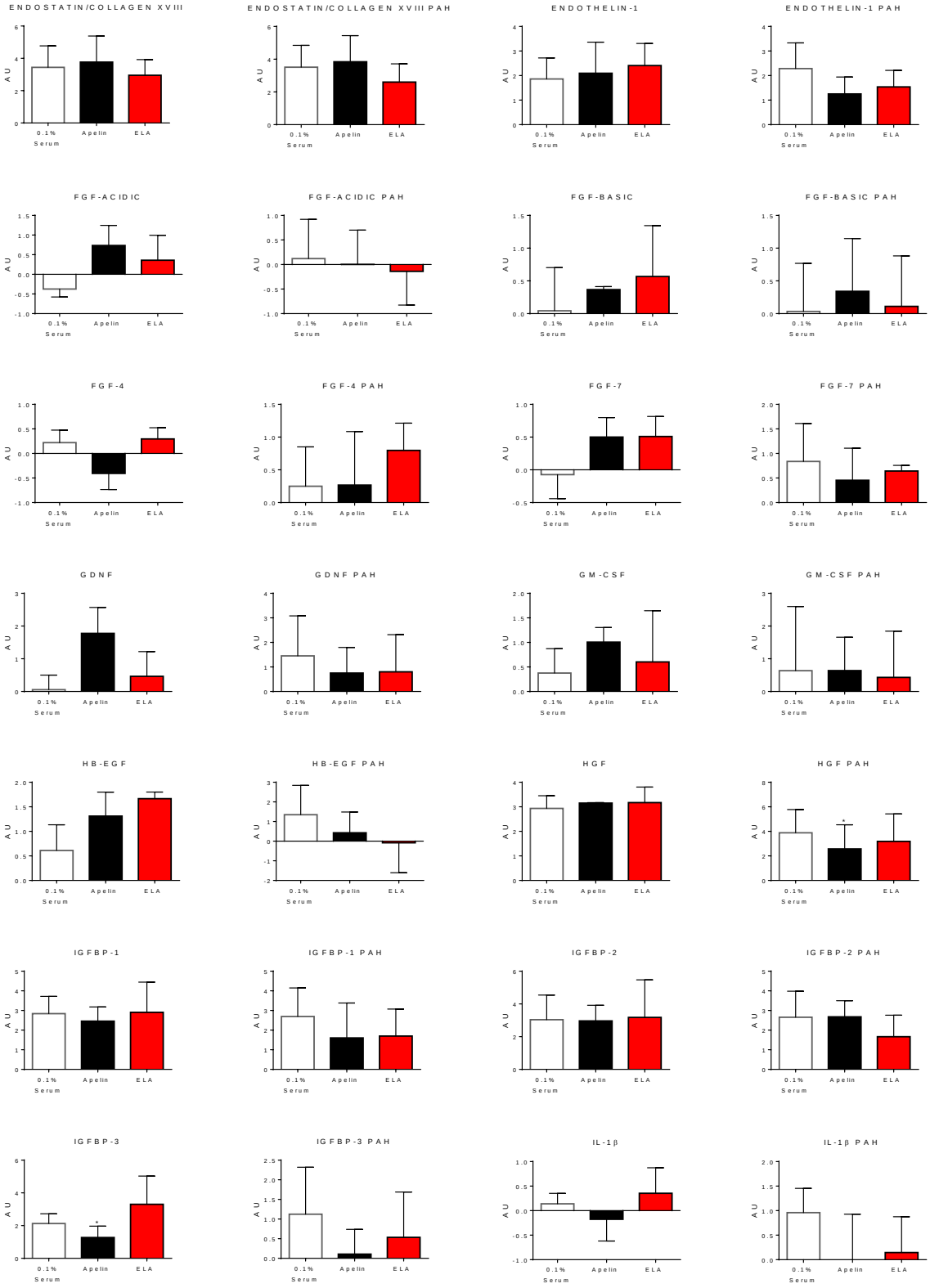

Supplemental Figure 5 continued.

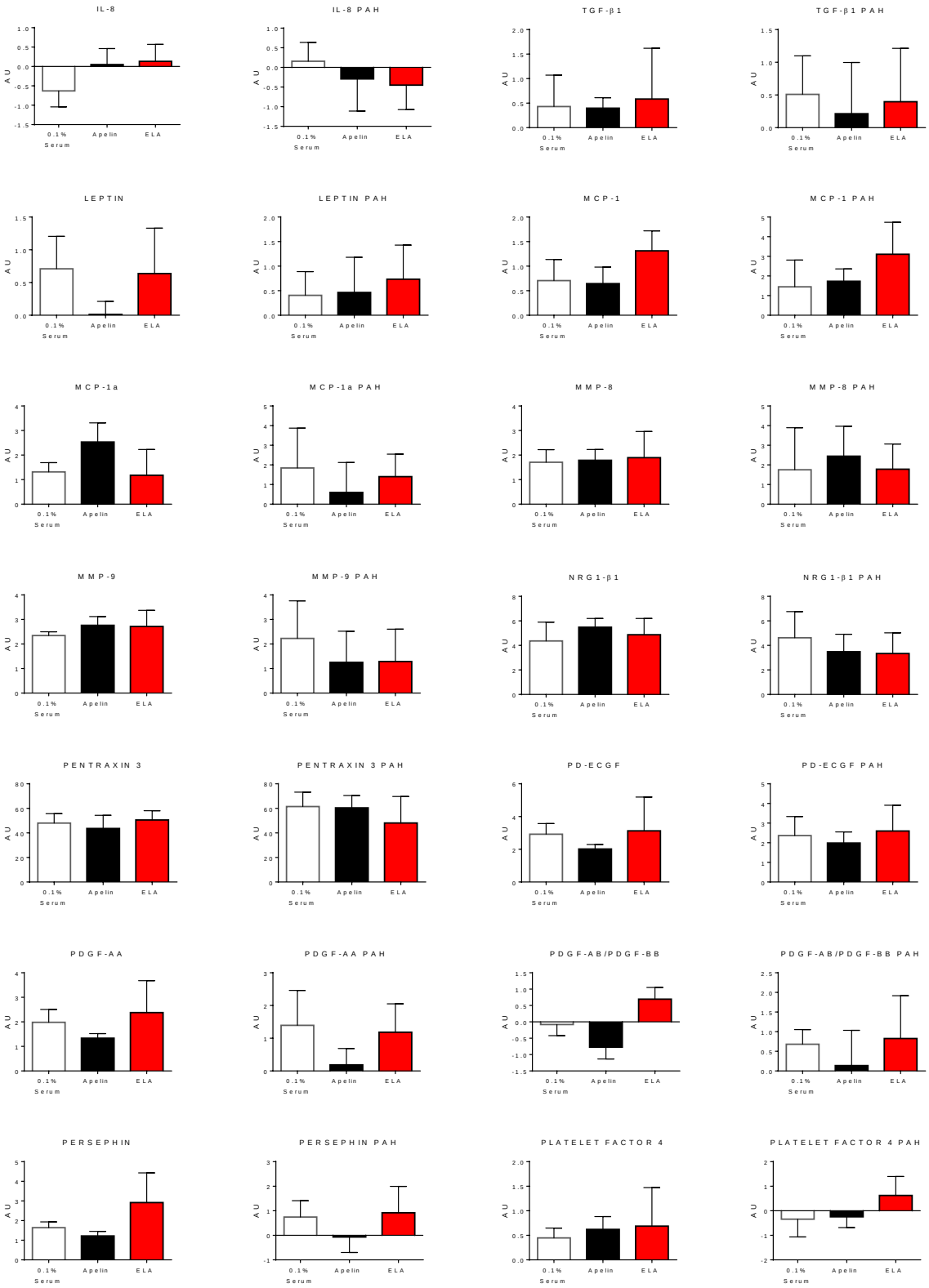

Supplemental Figure 5 continued.

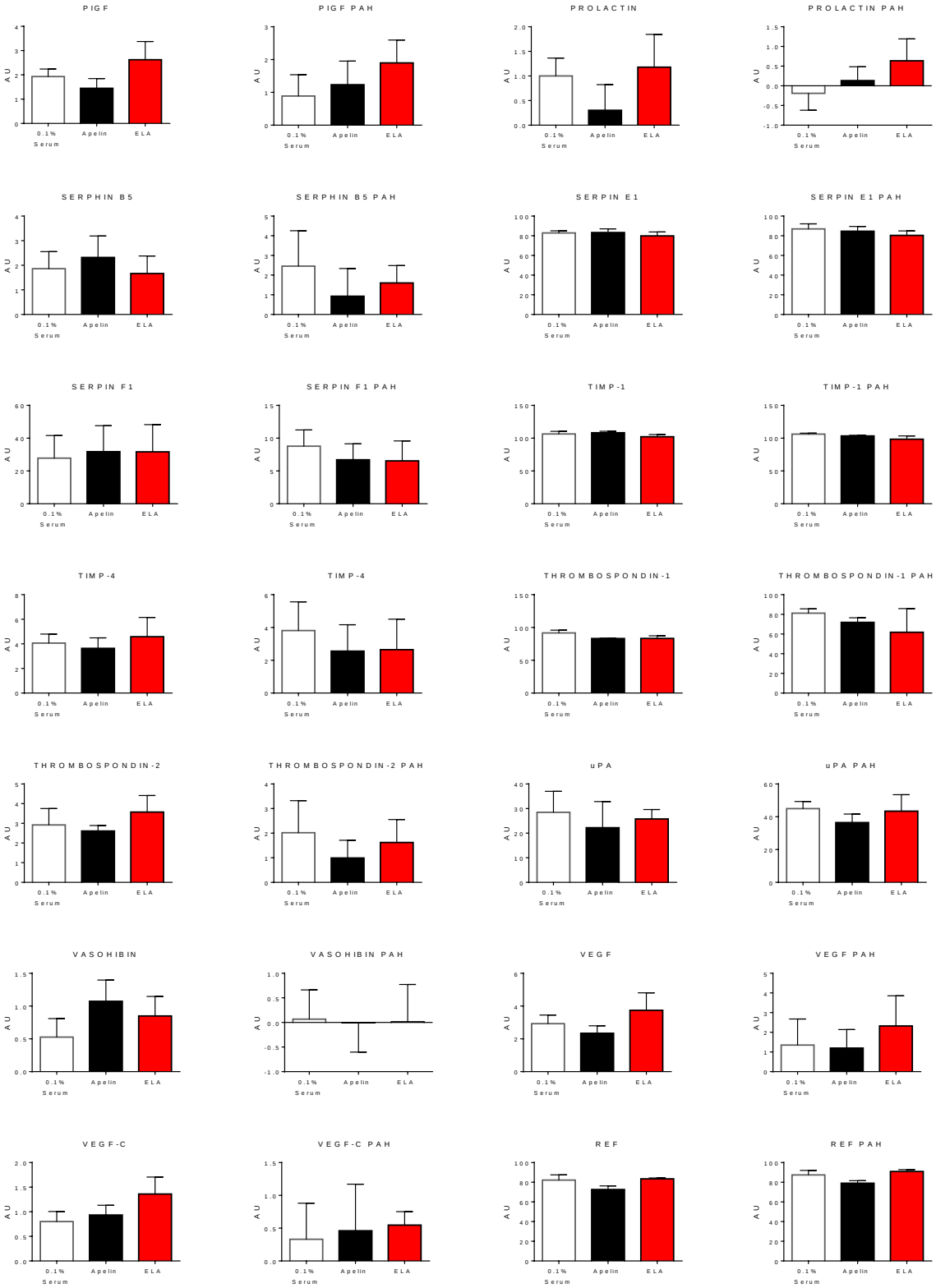

Expression of ELA in Human PAECs and Endothelium of Human Cardiovascular Tissues

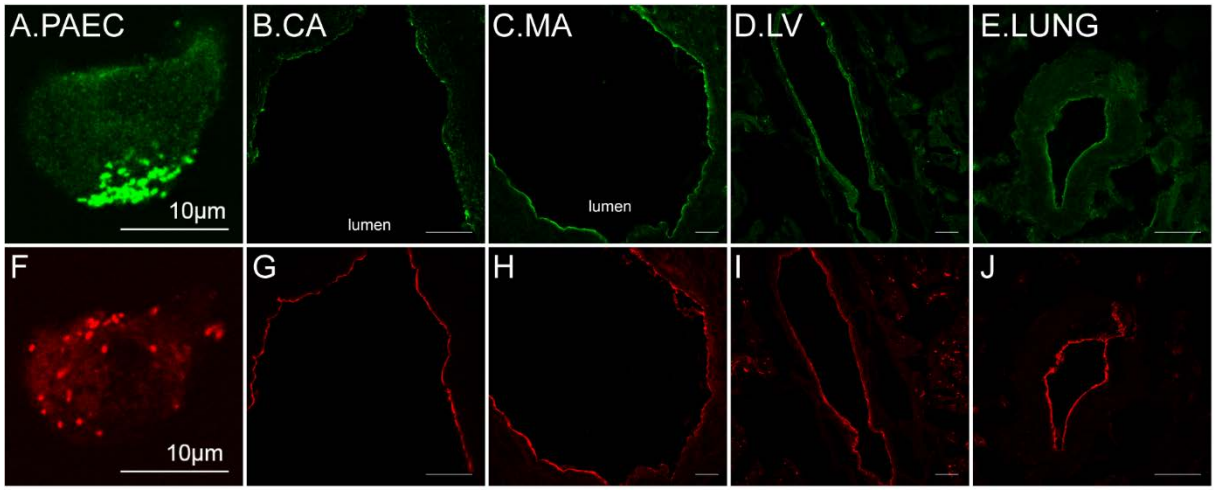

Supplemental Figure 6. Expression of ELA in human PAECs and endothelium of human cardiovascular tissues. Immunocytochemical localization of ELA-like immunoreactivity (green fluorescence) and vWF-like immunoreactivity in human (A, F) PAECs and endothelium of human (B, G), coronary artery (CA), (C, H) mammary artery (MA), (D, I) left ventricle (LV), (F, J) lung sections. Scale bars=75μm unless indicated.

Effects of ELA *in vivo*

There was no significant effect of ELA-32 and [Pyr^{1}]apelin-13 on heart rate in rat *in vivo*

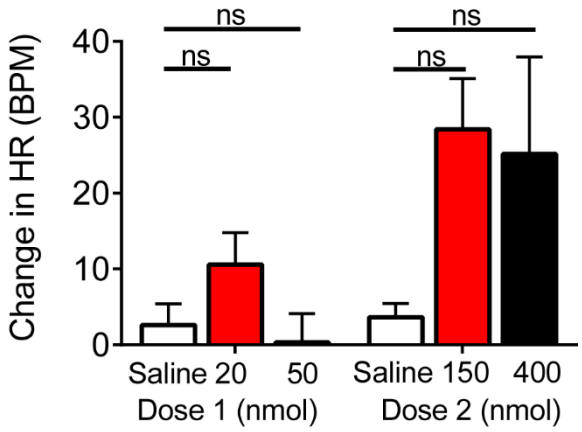

Supplemental Figure 7 The *in vivo* effects of increasing doses of ELA-32 (red bars) and [Pyr1]apelin-13 (black bars) on heart rate compared to saline controls (open bars). BPM, beats per minute.

Reduced Endothelial Staining of ELA in PAH Human Lung

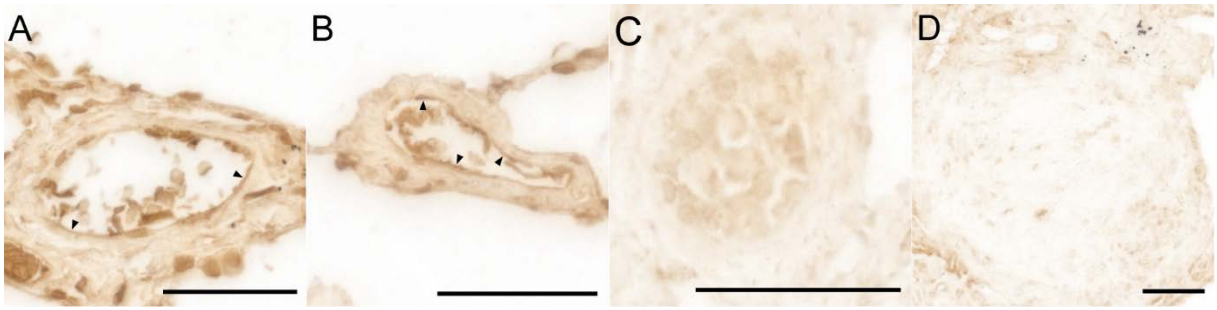

Supplemental Figure 8. Reduced endothelial ELA expression in human PAH lung. (A and B) Representative microphotographs of ELA-positive blood vessels (staining indicated by arrow heads) in a normal lung section. (C) Representative microphotograph showing ELA-negative blood vessels in a PAH lung section. (D) Representative microphotograph showing the absence of ELA-like immunoreacitivity in a pathological vascular lesion in a PAH lung section. Some non-specific staining due to red blood cell peroxidase are present as a useful marker of blood vessels. Scale bar=50μm.

Attenuation of Right Ventricular Hypertrophy by ELA in MCT Exposed Rat Heart

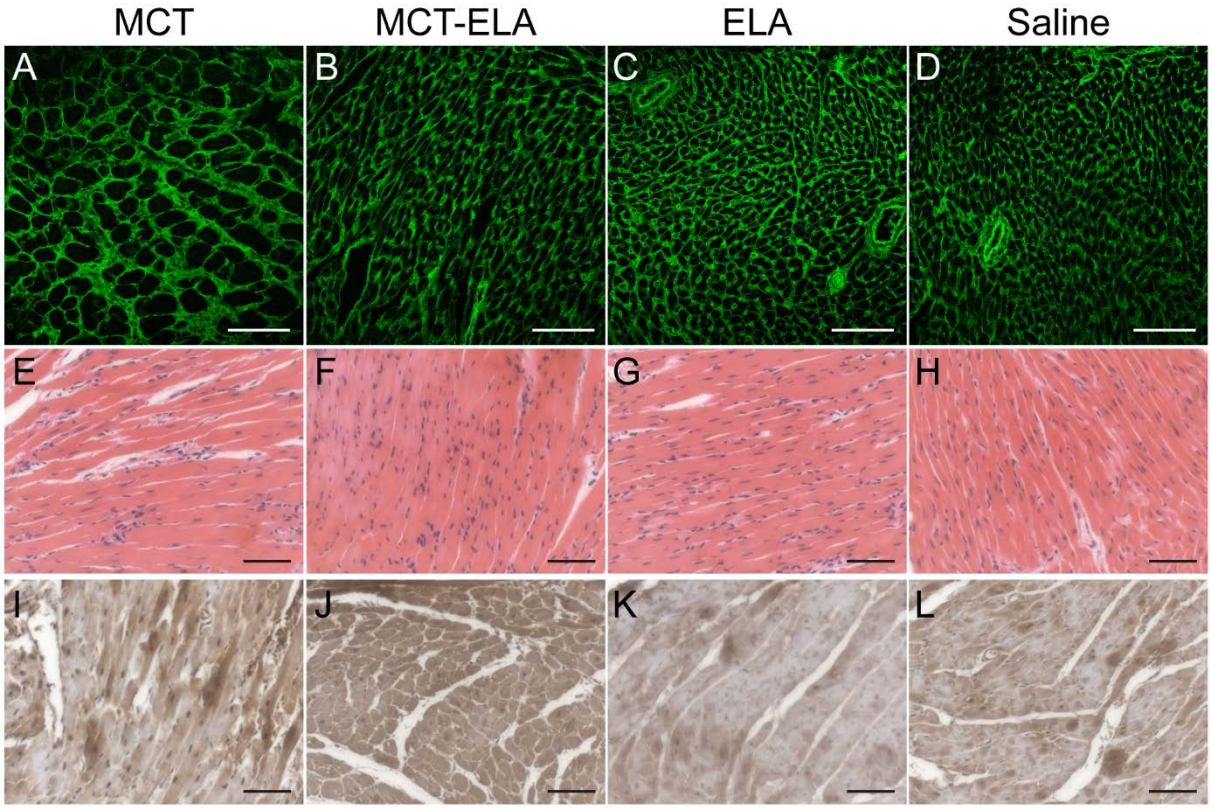

Supplemental Figure 9. Attenuation of right ventricular hypertrophy by ELA in MCT exposed rat heart. MCT exposure also resulted in significant RV hypertrophy indicated by (A) an increase in cardiomyocyte are (WGA staining), (E) a reduction in cardiomyocyte number/area (hematoxylin and eosin staining) and (I) an increase in the number of GATA4 positive nuclei/area compared to saline controls (D, H. L). There was a significant improvement in these following ELA-32 treatment of MCT exposed rats (B, F, J). ELA alone (C, G, K) had no significant effect compared to saline control. Scale bar = 75μm.

Lack of Significant Effect of Chronic Administration of ELA on Systemic Blood Pressure

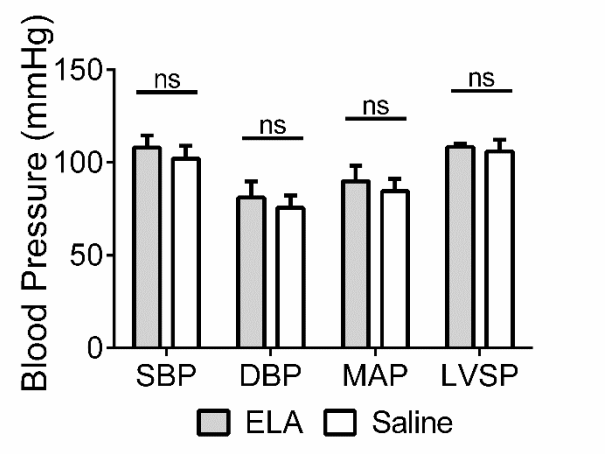

Supplemental Figure 10. Lack of significant effect of chronic administration of ELA on systemic blood pressure. 21 Days of ELA administration (n=5) did not affect systolic blood pressure (SBP), diastolica blood pressure (DBP), mean arterial pressure (MAP) or left ventricular systolic pressure (LVSP) compared to saline control (n=5).

No Significant Effect of ELA-32 Treatment on Plasma Levels of Angiotensin-II or BNP-32 Levels in Saline Control and MCT Exposed Rats.

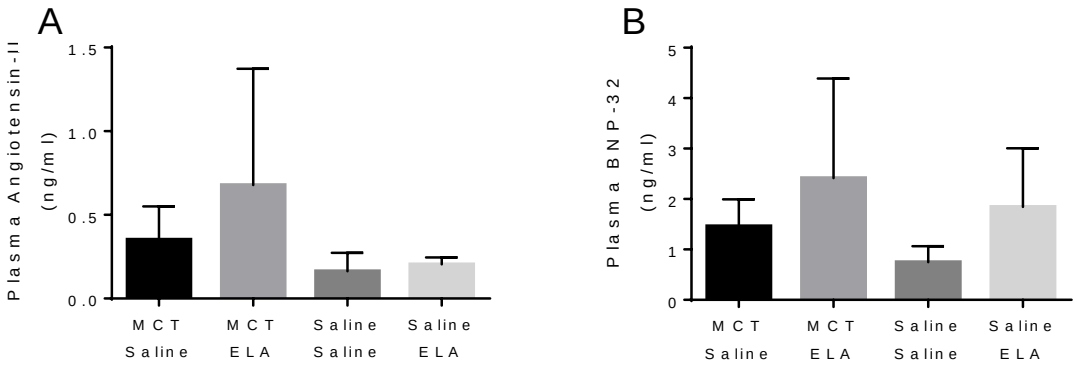

Supplemental Figure 11. Plasma levels of (A) angiotensin-II and (B) BNP-32 were not significantly affected by treatment with ELA-32 for 21 days in saline control or MCT exposed rats.

Supplemental References

1. Brame AL, Maguire JJ, Yang P, Dyson A, Torella R, Cheriyan J, Singer M, Glen RC, Wilkinson IB, Davenport AP. Design, characterization, and first-in-human study of the vascular actions of a novel biased apelin receptor agonist. *Hypertension*. 2015;65:834-840.
2. Wu B, Chien EY, Mol CD, Fenalti G, Liu W, Katritch V, Abagyan R, Brooun A, Wells P, Bi FC, Hamel DJ, Kuhn P, Handel TM, Cherezov V, Stevens RC. Structures of the CXCR4 chemokine GPCR with small-molecule and cyclic peptide antagonists. *Science.* 2010;330:1066-1071.
3. Sali A, Blundell TL. Comparative protein modelling by satisfaction of spatial restraints. *J Mol Biol.* 1993;234:779-815.
4. Sastry GM, Adzhigirey M, Day T, Annabhimoju R, Sherman W. Protein and ligand preparation: Parameters, protocols, and influence on virtual screening enrichments. *J Comput Aided Mol Des.* 2013;27:221-234.
5. Jones G, Willett P, Glen RC. Molecular recognition of receptor sites using a genetic algorithm with a description of desolvation. *J Mol Biol.* 1995;245:43-53.
6. Jones G, Willett P, Glen RC, Leach AR, Taylor R. Development and validation of a genetic algorithm for flexible docking. *J Mol Biol.* 1997;267:727-748.
7. Iturrioz X, Gerbier R, Leroux V, Alvear-Perez R, Maigret B, Llorens-Cortes C. By interacting with the C-terminal Phe of apelin, Phe255 and Trp259 in helix VI of the apelin receptor are critical for internalization. *J Biol Chem.* 2010;285:32627-32637.
8. Murza A, Sainsily X, Coquerel D, Côté J, Marx P, Besserer-Offroy É, Longpré JM, Lainé J, Reversade B, Salvail D, Leduc R, Dumaine R, Lesur O, Auger-Messier M, Sarret P, Marsault É. Discovery and structure-activity relationship of a bioactive fragment of elabela that modulates vascular and cardiac functions. *J Med Chem.* 2016;59:2962-2972.

9. Clark AM, Labute P, Santavy M. 2D structure depiction. *J Chem Inf Model.* 2006;46:1107-1123

10. Maloney PR, Khan P, Hedrick M, Gosalia P, Milewski M, Li L, Roth GP, Sergienko E, Suyama E, Sugarman E, Nguyen K, Mehta A, Vasile S, Su Y, Stonich D, Nguyen H, Zeng FY, Novo AM, Vicchiarelli M, Diwan J, Chung TD, Smith LH, Pinkerton AB. Discovery of 4-oxo-6-((pyrimidin-2-ylthio)methyl)-4h-pyran-3-yl 4-nitrobenzoate (ML221) as a functional antagonist of the apelin (APJ) receptor. *Bioorg Med Chem Lett.* 2012;22:6656-6660.

11. Schmittgen TD, Livak KJ. Analyzing real-time PCR data by the comparative C(T) method. *Nat Protoc.* 2008;3:1101-1108.

12. Kleinz MJ, Davenport AP. Immunocytochemical localization of the endogenous vasoactive peptide apelin to human vascular and endocardial endothelial cells. *Regul Pept.* 2004;118:119-125.

13. Schneider CA, Rasband WS, Eliceiri KW. NIH image to ImageJ: 25 years of image analysis. *Nat Methods.* 2012;9:671-675.

14. Schindelin J, Arganda-Carreras I, Frise E, Kaynig V, Longair M, Pietzsch T, Preibisch S, Rueden C, Saalfeld S, Schmid B, Tinevez JY, White DJ, Hartenstein V, Eliceiri K, Tomancak P, Cardona A. Fiji: An open-source platform for biological-image analysis. *Nat Methods.* 2012;9:676-682.

15. Moseley EL, Atkinson C, Sharples LD, Wallwork J, Goddard MJ. Deposition of C4d and C3d in cardiac transplants: A factor in the development of coronary artery vasculopathy. *J Heart Lung Transplant.* 2010;29:417-423.

16. Chandra SM, Razavi H, Kim J, Agrawal R, Kundu RK, de Jesus Perez V, Zamanian RT, Quertermous T, Chun HJ. Disruption of the apelin-APJ system worsens hypoxia-induced pulmonary hypertension. *Arterioscler Thromb Vasc Biol.* 2011;31:814-820.

17. Buonincontri G, Methner C, Carpenter TA, Hawkes RC, Sawiak SJ, Krieg T. MRI and PET in mouse models of myocardial infarction. *J Vis Exp.* 2013;e50806:1-9.

18. Heiberg E, Sjögren J, Ugander M, Carlsson M, Engblom H, Arheden H. Design and validation of Segment--freely available software for cardiovascular image analysis. *BMC Med Imaging.* 2010;10:1-13.

19. Pacher P, Nagayama T, Mukhopadhyay P, Bátkai S, Kass DA. Measurement of cardiac function using pressure-volume conductance catheter technique in mice and rats. *Nat Protoc.* 2008;3:1422-1434.

20. LaCroix C, Freeling J, Giles A, Wess J, Li YF. Deficiency of M2 muscarinic acetylcholine receptors increases susceptibility of ventricular function to chronic adrenergic stress. *Am J Physiol Heart Circ Physiol.* 2008;294:H810-820.

21. Long L, Ormiston ML, Yang X, Southwood M, Gräf S, Machado RD, Mueller M, Kinzel B, Yung LM, Wilkinson JM, Moore SD, Drake KM, Aldred MA, Yu PB, Upton PD, Morrell NW. Selective enhancement of endothelial BMPR-II with BMP9 reverses pulmonary arterial hypertension. *Nat Med.* 2015;21:777-785.

22. Crosby A, Soon E, Jones FM, Southwood MR, Haghighat L, Toshner MR, Raine T, Horan I, Yang P, Moore S, Ferrer E, Wright P, Ormiston ML, White RJ, Haight DA, Dunne DW, Morrell NW. Hepatic Shunting of Eggs and Pulmonary Vascular Remodeling in Bmpr2(+/-) Mice with Schistosomiasis. *Am J Respir Crit Care Med.* 2015;192:1355-1365.

23. Oka T, Maillet M, Watt AJ, Schwartz RJ, Aronow BJ, Duncan SA, Molkentin JD. Cardiac-specific deletion of Gata4 reveals its requirement for hypertrophy, compensation, and myocyte viability. *Circ Res.* 2006;98:837-845.

Supplemental Video 1: The effect of ELA-32 on the rat heart *in vivo*. Mid-ventricular transverse view acquired using MRI with first video was taken at baseline and six subsequent time points within 10 minutes following the intravenous injection of ELA-32.

Supplemental Video 2: The effect of [Pyr^{1}]apelin-13 on the rat heart *in vivo*. Mid-ventricular transverse view acquired using MRI with first video was taken at baseline and six subsequent time points within 10 minutes following the intravenous injection of [Pyr^{1}]apelin-13.